



Department of
Electrical & Electronics Engineering
Abdullah Gül University

Project Report for Electrostatic Energy in Ionic Crystals



Department of
Electrical & Electronics Engineering
Abdullah Gül University

Project Report

EE1100 ESD Capsule

Submitted on: 21.05.2023

Submitted by: Sümeyye YILDIRIM

GROUP MEMBERS

SÜMEYYE YILDIRIM

AHMED ABDELNASER

MEHMET FATİH GÖĞÜŞ

OBJECTIVE

The purpose of this experiment is to understand electrostatic energy in NaCl crystal as shown in Figure 1 and Van Der Walls bonding for inert gas crystals as shown in Figure 2. Analyzing the interactions and potential energy associated with electric charges is the goal of researching electrostatic energy in multi-particle systems. Our goal is to comprehend the behavior and equilibrium of charged particles in complicated systems by looking into Coulomb's law, which regulates the force between charges, and the idea of electrostatic potential energy.

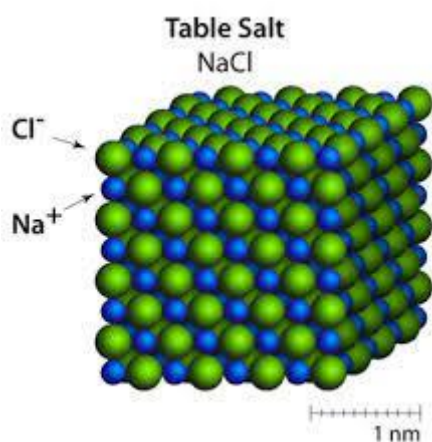


FIGURE 1

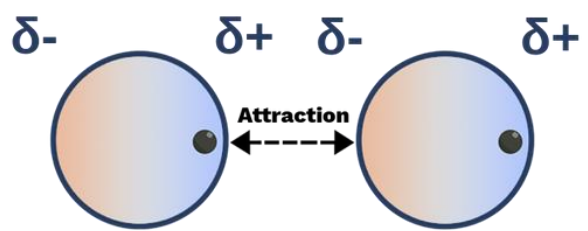


FIGURE 2

The potential energy in multi-particle systems is the total of all pairwise interactions between every pair of charged particles. We may assess the electrostatic potential energy, indicated as U , for a system with n charges through careful research and computations. This energy calculation takes into account the magnitudes of the charges, their separations, and the electrostatic constant. We are able to determine the system's stability and equilibrium by looking at the total potential energy. The system is in equilibrium and the total potential energy is at its lowest value when forces between charges balance each other out.

Understanding the special interactions and forces that control the stability and characteristics of these crystalline structures is the main goal of research on Van der Waals (molecular) bonding in inert gas crystals. Helium, neon, argon, krypton, and xenon are examples of inert gases, which are distinguished by their low reactivity and resistance to forming chemical bonds. Due to their full electron shells, these noble gases often do not readily engage in conventional bonding processes like ionic or covalent bonding. These gases can, however, condense into solid, crystalline forms that are held together by Van der Waals forces in appropriate situations, such as extremely low temperatures and high pressures.

To better understand this question, the Lennard Jones potential energy equation was used. Understanding the intermolecular interactions and potential energy between neutral atoms or molecules in a variety of settings is the goal of studying the Lennard-Jones potential. An approximate mathematical representation of the interatomic or intermolecular potential energy as a function of distance is the Lennard-Jones potential. It is frequently used to describe the attractive and repulsive forces between particles in theoretical research and molecular simulations.

The Lennard-Jones potential has two parts: a word for the attractive interactions between particles, which decrease with distance, and a term for the repulsive forces, which abruptly rise as particles get too close to one another. The stability and behavior of the system are determined by how these attracting and repellent forces interact.

BACKGROUND

An analytical series is generated for the electrical potential energy in a 1-dimensional NaCl crystal. This is the sum of the infinite series. Thanks to the total structure, the Madelung coefficient is found. The same process is repeated in 2 dimensions that are more complex than 1 dimension. An analytical series is obtained for the electrical potential energy of the 2-dimensional NaCl crystal, and in addition, a numerical evaluation is made for the Madelung constant.

A resistor network with 4, 16, 64, 128 and 256 nodes are created using a simulation tool. The equivalent resistance of the created network is calculated. As the number of nodes increases, comments are made on how the result of the equivalent resistance changes and the result of the equivalent resistance. Then a resistive network consisting of 4 and 16 nodes made of the resistors of our choice is created in the laboratory environment. The equivalent resistance of this network created in a laboratory environment is determined using a test method. The results obtained using the simulation tool are compared with the results obtained in the laboratory environment.

Using a simulation tool, a capacitor network with 4, 16, 64, 128 and 256 nodes is built. Calculations are made to determine the network's equivalent capacitance. Comments are made regarding how the equivalent capacitance result varies as the number of nodes rises as well as the equivalent capacitance result. The capacitors we have selected are then used in the laboratory to build a capacitive network with 4 to 16 nodes. Using a test method, the equivalent capacitance of this network built in a lab setting is ascertained. The outcomes produced by the simulation tool are contrasted with those produced in a laboratory setting.

In addition, comments are made on how the toy model, which is the model that provides a simplified understanding of how electrons move and interact with the lattice in a metal or semiconductor, causing electrical resistance. Arguments are made on how temperature affects vibrations.

ANALYTICAL AND SIMULATION PROCEDURES

a. Steps of Experiment

In this project

- LTSPICE
- MATLAB
- Resistors
- Capacitors
- Multimeter
- Breadboard

are used.

1. Each ion in an endless linear chain interacts with its neighboring ions through electrostatic forces. Coulomb's law, which states that the potential energy is directly proportional to the product of the charges and inversely proportional to the distance between them, determines the electrostatic potential energy between two ions. A sodium ion is chosen as a reference. The equation of the electrostatic potential energy in the infinite linear chain of ions is developed. An analytical series is produced for electrostatic potential energy.
2. An electrostatic potential energy series is produced for infinite ion pairs in 1 dimension. Madelung's constant of the obtained series is found when necessary operations are done.
3. It is written the equation for the electrostatic potential energy of the NaCl salt crystal for 2 dimensions that are more complex than 1 dimension. Again, an analytical series is produced for this equation. A numerical evaluation is made for the Madelung constant for a 2-dimensional crystal.
4. A simulation tool is utilized to create resistor networks with 4, 16, 64, 128, and 256 nodes. The primary objective is to determine the equivalent resistance of each network. By analyzing the results, observations can be made regarding how the equivalent resistance changes as the number of nodes increases.
5. In the laboratory setting, resistive networks comprising 4 and 16 nodes are constructed using selected resistors. The objective is to measure the equivalent resistance of these networks using a test method specific to the laboratory environment. By doing so, a comparison can be made between the results obtained from the simulation tool and the experimental measurements carried out in the laboratory. This analysis enables an assessment of the agreement or disparity between the simulated and real-world equivalent resistance values.

6. A simulation tool is employed to construct a capacitor network with varying numbers of nodes: 4, 16, 64, 128, and 256. The purpose is to calculate the equivalent capacitance of each network and observe how this value changes with increasing node count. By analyzing the results, comments can be made regarding the relationship between the number of nodes and the resulting equivalent capacitance value.
7. The selected capacitors are employed in the laboratory to construct a capacitive network ranging from 4 to 16 nodes. Through a specific test method, the equivalent capacitance of this network, created in the laboratory environment, is determined. Subsequently, a comparison is made between the results obtained from the simulation tool and the experimental measurements conducted in the laboratory. This comparison serves to assess the agreement or discrepancy between the equivalent capacitance values obtained through simulation and those obtained in the real-world laboratory setting.
8. An equation is derived for the force F between particles based on the Lennard-Jones potential equation, which describes the intermolecular or interatomic interactions. This equation relates the force to the distance between the particles, denoted as r .
9. Extremum (minimum and maximum) properties for $U(r)$ and $F(r)$ functions are searched and graphs of both functions are drawn.
10. The equilibrium distance, r_{eq} , for the Lennard-Jones potential has been discovered.
11. The equation of the force F_x, F_y, F_z is written in Cartesian coordinates, taking into account its spherical symmetry with respect to the radial measure r of this force.
12. The Cartesian components of the gradient vector for the potential energy function $U(r)$ have been determined.
13. The work, denoted as W , required to transfer an electrical charge of magnitude e from the initial position at $r = \sigma$ to an infinite distance by the Lennard-Jones force has been determined.
14. Observations and insights are provided regarding the toy model, which offers a simplified representation of how electrons move and interact with the lattice structure in a metal or semiconductor, leading to electrical resistance. Arguments are presented on how temperature influences the vibrations within the lattice and their impact on electron behavior.

EVALUATION OF PROBLEMS

Part 1

Ions with positive and negative charges form the amazing structure of ionic crystals like NaCl in Figure 3. We can think of these ions as solid spheres with electric charges. Electrostatic forces, which powerfully attract positive ions to negative ions and vice versa, are what essentially control how they interact. The attractive forces between these ions become stronger as they go closer to one another, thereby lowering the potential energy. But eventually, the ion spheres approach each other and come into contact. A strong repulsive force that originates from the overlapping electron clouds that surround the ions emerges at this crucial distance. The ions can't go much closer because of the repelling force acting as a barrier. In fact, as the repulsive force increases quickly, trying to get the ions closer together gets harder and harder. Strong resistance to compression results from what appears to be the formation of an unseen wall between the ions. Thus, the intricate interplay between attractive and repulsive forces in an ionic crystal like NaCl provides stability to its lattice structure. This delicate balance ensures that the crystal maintains its integrity, preventing the ions from collapsing onto each other and resulting in a solid, rigid arrangement.

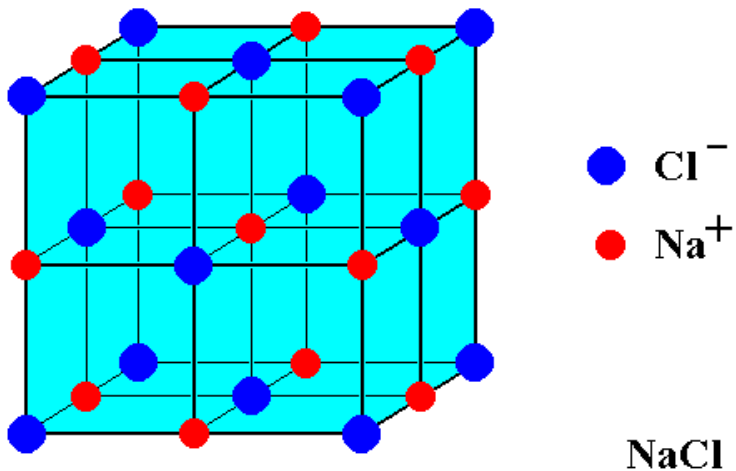


FIGURE 3

The Madelung constant, an essential factor in comprehending the characteristics and stability of ionic solids, is a mathematical constant employed for determining the electrostatic potential energy within an ionic crystal lattice. This constant is obtained by summing up the electrostatic potentials generated by individual ions in the crystal lattice while considering their respective charges and relative positions. It encapsulates the combined influence of long-range Coulombic interactions among the ions constituting the crystal. The numerical value of the Madelung constant is contingent upon the particular crystal structure and the spatial arrangement of the ions within it.

To find Madelung constant for 1D NaCl crystal as shown in Figure 4 with $R_e = 2.81 \times 10^{-8} \text{ cm}$, the following procedures are applied:

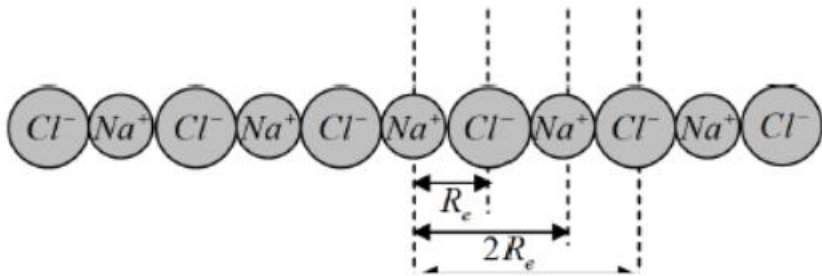


FIGURE 4

To find the Madelung constant (a), the electrostatic potential energy must be calculated. The general formula for electrostatic potential energy is as follows.

$$U = -a \frac{q^2}{4\pi\epsilon_0 R_e}$$

a = Madelung constant

q = electrical charge (The ions in the crystal possess electrical charges (q) that are equivalent to the charge of an electron (e).)

ϵ_0 = permittivity of free space

R_e = distance between centers of ions

Let's take sodium ion as a reference ion.

First Shell: Na^+ has two Cl^- ions as its nearest neighbors.

The electrical potential energy that the sodium ion has because of the chlorine atom to its left is as follows:

$$\frac{-e^2}{4\pi\epsilon_0 R_e}$$

The electrical potential energy that the sodium ion has because of the chlorine atom to its right is as follows:

$$\frac{-e^2}{4\pi\epsilon_0 R_e}$$

So, the electrical potential energy is:

$$\frac{-e^2}{4\pi\epsilon_0 R_e} + \frac{-e^2}{4\pi\epsilon_0 R_e} = \frac{-2e^2}{4\pi\epsilon_0 R_e}$$

Second Shell: This time there are two Na^+ ions with $2R_e$ distance.

The electrical potential energy that the sodium ion has because of the sodium atom to its left is as follows:

$$\frac{+e^2}{4\pi\epsilon_0 2R_e}$$

The electrical potential energy that the sodium ion has because of the sodium atom to its right is as follows:

$$\frac{+e^2}{4\pi\epsilon_0 2R_e}$$

So, the electrical potential energy is:

$$\frac{+e^2}{4\pi\epsilon_0 2R_e} + \frac{+e^2}{4\pi\epsilon_0 2R_e} = \frac{+2e^2}{4\pi\epsilon_0 2R_e}$$

Third Shell: There are two Cl^- ions with $3R_e$ distance.

$$\frac{-e^2}{4\pi\epsilon_0 3R_e} + \frac{-e^2}{4\pi\epsilon_0 3R_e} = \frac{-2e^2}{4\pi\epsilon_0 3R_e}$$

Fourth Shell: There are two Na^+ ions with $4R_e$ distance.

$$\frac{+e^2}{4\pi\epsilon_0 4R_e} + \frac{+e^2}{4\pi\epsilon_0 4R_e} = \frac{+2e^2}{4\pi\epsilon_0 4R_e}$$

...

...

...

These operations are also done for other shells and so on. Assuming the general idea is understood, the total energy can be written as:

$$U_{total} = \frac{-2e^2}{4\pi\varepsilon_0 R_e} + \frac{2e^2}{4\pi\varepsilon_0 2R_e} - \frac{2e^2}{4\pi\varepsilon_0 3R_e} + \frac{2e^2}{4\pi\varepsilon_0 4R_e} - \dots$$

Necessary simplifications are made:

$$U_{total} = \frac{2e^2}{4\pi\varepsilon_0 R_e} \left(-1 + \frac{1}{2} - \frac{1}{3} + \frac{1}{4} - \dots \right)$$

$$U_{total} = \frac{-2e^2}{4\pi\varepsilon_0 R_e} \left(1 - \frac{1}{2} + \frac{1}{3} - \frac{1}{4} + \dots \right)$$

For the continuation of the question, help is taken from the Maclaurin series:

$$\ln(1+x) = \sum (-1)^{n+1} \frac{x^n}{n} = x - \frac{x^2}{2} + \frac{x^3}{3} - \frac{x^4}{4} + \dots$$

It is seen that there is a similarity between the series whose general expression is shown above and $(1 - \frac{1}{2} + \frac{1}{3} - \frac{1}{4} + \dots)$. Since it is obvious, the x value is 1.

$$U_{total} = \frac{-2e^2}{4\pi\varepsilon_0 R_e} (\ln 2)$$

$$U_{total} = -2 \ln 2 \frac{e^2}{4\pi\varepsilon_0 R_e}$$

$$U_{total} = -2 \ln 2 \frac{e^2}{4\pi(8.85 \times 10^{-12})(2.81 \times 10^{-10} m)}$$

$$a = 2 \ln 2$$

$$a = 1.386294361 \quad a \cong 1.38$$

The procedures for numerical evaluation of Madelung's constant α for a 2-dimensional infinite NaCl crystal in Figure 5 are as follows:

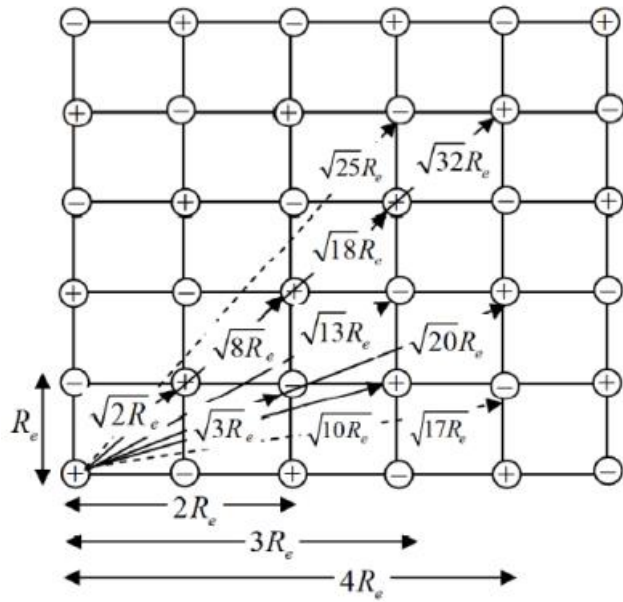


FIGURE 5

Na^+ ion which is placed in the corner is chosen as a reference. The general formula of electrical potential energy was like that:

$$U = -a \frac{q^2}{4\pi\epsilon_0 R_e}$$

First Nearest: The closest distance to this sodium ion is at R_e . At a distance of R_e , there are 4 Cl^- ions. So, the electrical potential energy is:

$$\frac{-4e^2}{4\pi\epsilon_0 R_e}$$

It is $4e^2$ because there are four chloride ions. And the distance was R_e .

Next Nearest: The nearest distance after R_e is $\sqrt{2}R_e$. At a distance of $\sqrt{2}R_e$, there are 4 Na^+ ions. So, the electrical potential energy is:

$$\frac{+4e^2}{4\pi\epsilon_0 \sqrt{2}R_e}$$

It is $4e^2$ because there are four sodium ions. And the distance was $\sqrt{2}R_e$.

Next Nearest: The nearest distance after $\sqrt{2}R_e$ is $2R_e$. at a distance of $2R_e$, there are 4 Na^+ ions.

$$\frac{+4e^2}{4\pi\epsilon_0 2R_e}$$

Next Nearest: This time the distance is $\sqrt{5}R_e$. There are 8 chloride ions.

$$\frac{-8e^2}{4\pi\epsilon_0 \sqrt{5}R_e}$$

Next Nearest: This time the distance is $\sqrt{8}R_e$. There are 4 sodium ions.

$$\frac{+4e^2}{4\pi\epsilon_0 \sqrt{8}R_e}$$

Next Nearest: This time the distance is $3R_e$. There are 4 chloride ions.

$$\frac{-4e^2}{4\pi\epsilon_0 3R_e}$$

Next Nearest: This time the distance is $\sqrt{10}R_e$. There are 8 sodium ions.

$$\frac{+8e^2}{4\pi\epsilon_0 \sqrt{10}R_e}$$

Next Nearest: This time the distance is $\sqrt{13}R_e$. There are 8 chloride ions.

$$\frac{-8e^2}{4\pi\epsilon_0 \sqrt{13}R_e}$$

Next Nearest: This time the distance is $4R_e$. There are 4 sodium ions.

$$\frac{+4e^2}{4\pi\epsilon_0 4R_e}$$

...

...

...

This is how these processes go. These operations are also done for other ions and distances. Assuming the general idea is understood, the total energy can be written as:

$$U_{total} = \frac{-4e^2}{4\pi\epsilon_0 R_e} + \frac{+4e^2}{4\pi\epsilon_0 \sqrt{2}R_e} + \frac{+4e^2}{4\pi\epsilon_0 2R_e} + \frac{-8e^2}{4\pi\epsilon_0 \sqrt{5}R_e} + \frac{+4e^2}{4\pi\epsilon_0 \sqrt{8}R_e} + \frac{-4e^2}{4\pi\epsilon_0 3R_e} + \\ \frac{+8e^2}{4\pi\epsilon_0 \sqrt{10}R_e} + \frac{-8e^2}{4\pi\epsilon_0 \sqrt{13}R_e} + \frac{+4e^2}{4\pi\epsilon_0 4R_e} + \dots$$

$$U_{total} = \frac{-e^2}{4\pi\epsilon_0 R_e} \left(4 - \frac{4}{\sqrt{2}} - \frac{4}{2} + \frac{8}{\sqrt{5}} - \frac{4}{\sqrt{8}} + \frac{4}{3} - \frac{8}{\sqrt{10}} + \frac{8}{\sqrt{13}} - \frac{4}{4} + \dots \right)$$

$$U_{total} = \frac{-e^2}{4\pi\epsilon_0 R_e} (1.3571 + \dots)$$

$$U_{total} = -(1.3571 + \dots) \frac{e^2}{4\pi\epsilon_0 R_e}$$

$$a = (1.3571 + \dots)$$

An exact Madelung constant was reached for the 1-dimensional NaCl crystal. However, as can be seen, a definite Madelung constant for the 2-dimensional crystal could not be reached. It was anticipated that we would arrive at such a conclusion. That's why it was called to make the numerical evaluation of Madelung constant in the question.

Traditional methods using the parallel and series resistor equations are easy in estimating the equivalent resistance of resistors. However, when dealing with a large number of resistors, such as 16, 64, 128, or 256, calculating the equivalent resistance becomes significantly more difficult. In order to escape this hard obstacle, the employment of LTSPICE, a powerful circuit simulation software, comes to our aid.

FOR 4 NODES

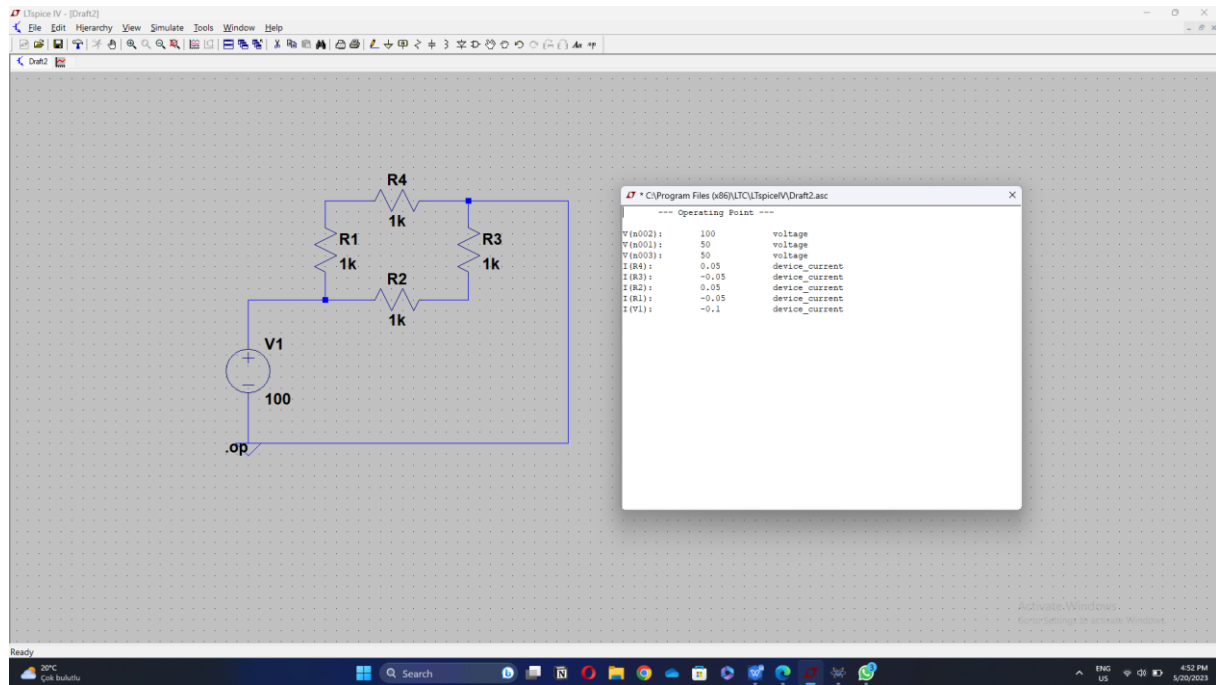


FIGURE 6

By configuring the resistors within a voltage circuit, as depicted in Figure 6, we can acquire the current flowing through the equivalent resistance of the resistors. Subsequently, employing the equation governing the current within a resistor, we can decide the value of the equivalent resistance.

$$R_{eq} = \frac{V}{I}$$

V : The voltage of the circuit .

R_{eq} : The equivalent resistance .

I : The current of the circuit .

$$R_{eq} = \frac{V}{I} = \frac{100V}{0.1A} = 1k\Omega$$

FOR 16 NODES

As shown in figure 7, we will do the same steps to find the equivalent resistance of 16 node resistor :

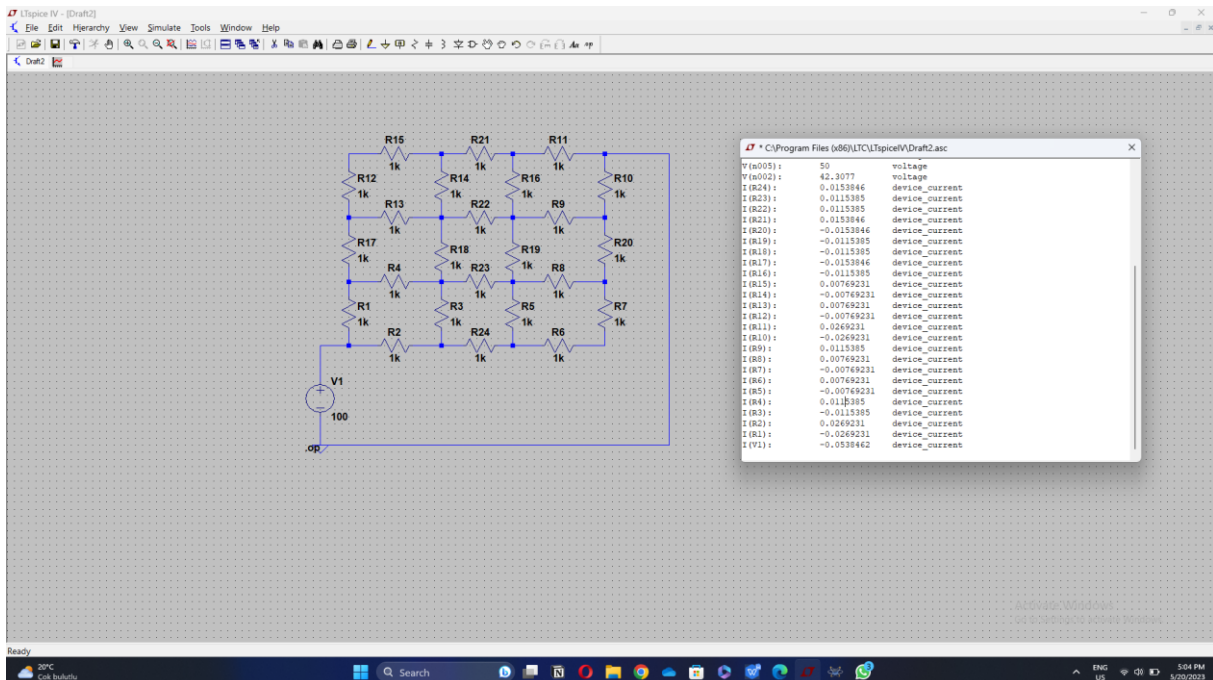


FIGURE 7

$$R_{eq} = \frac{V}{I} = \frac{100V}{0.0538A} = 1.859k\Omega$$

FOR 64 NODES

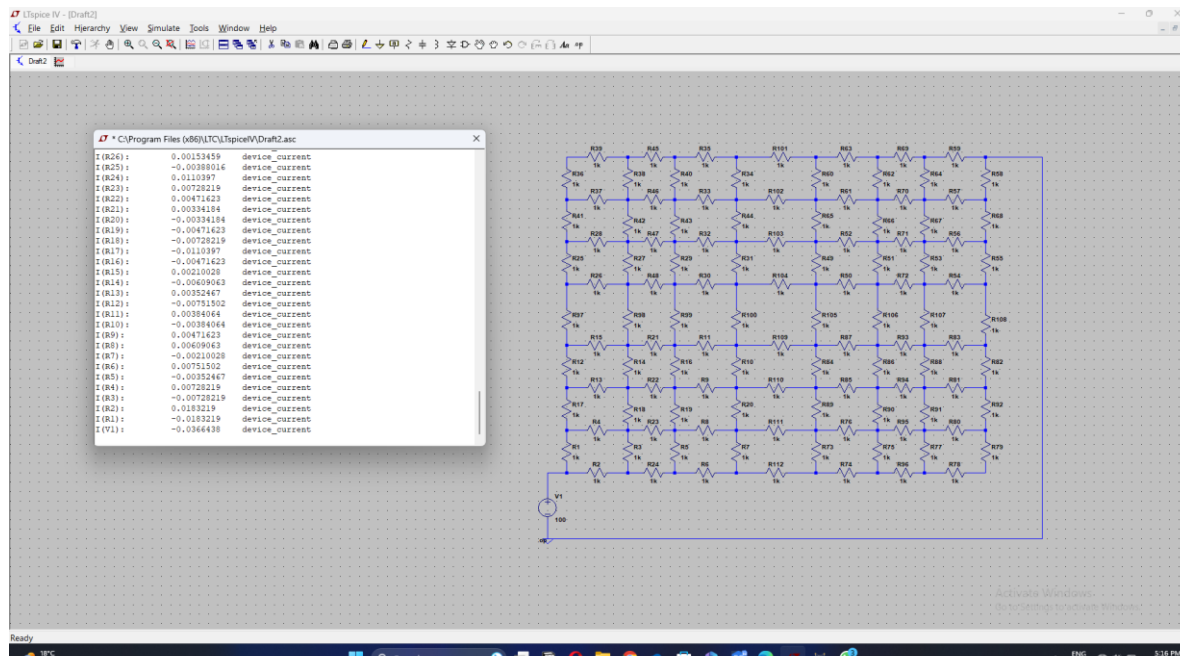


FIGURE 8

$$R_{eq} = \frac{V}{I} = \frac{100V}{0.03664A} = 2.729k$$

FOR 128 NODES

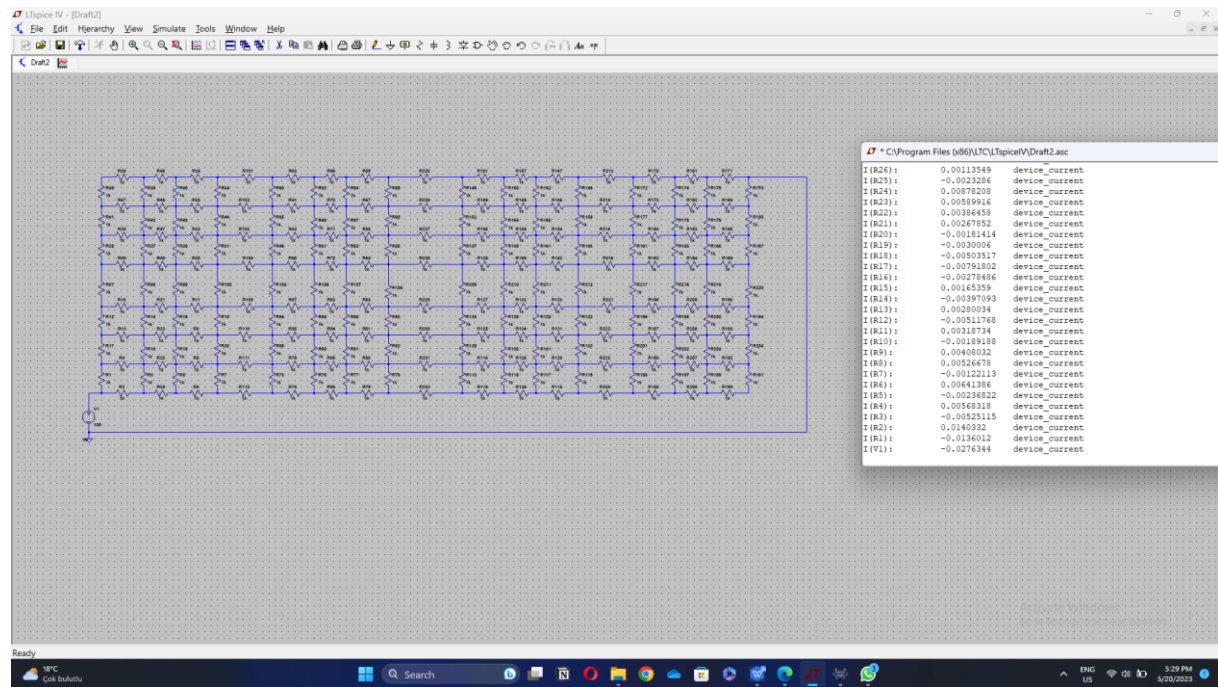


FIGURE 9

$$R_{eq} = \frac{V}{I} = \frac{100V}{0.0276A} = 3.623k\Omega$$

FOR 256 NODES

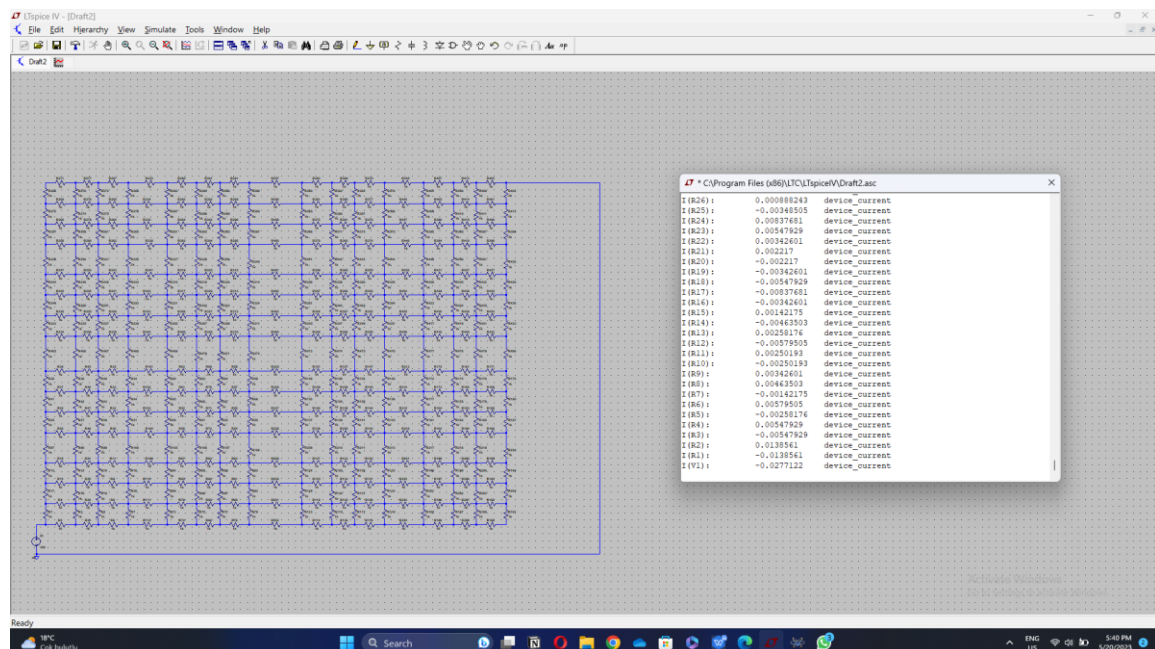


FIGURE 9

$$R_{eq} = \frac{V}{I} = \frac{100}{0.0277} = 3.610\text{k}\Omega$$

When the resistances of each node are evaluated, an unusual pattern develops in which the currents of each node follow a distinctive parabolic curve pattern. It is important to remember that the equation describing the connection between current and resistance states that a rise in resistance results in a fall in current. As a result, we might conclude that the equivalent resistance of each node follows also a parabolic trend, as seen in the figures.

A resistive network of 4 and 16 nodes is created made of the resistors of our choice. A test method is developed to measure the equivalent resistance. The actions taken will be shown below.

FOR 4 NODES

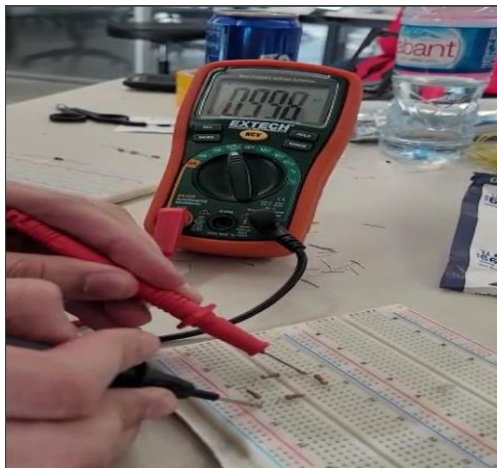


FIGURE 10

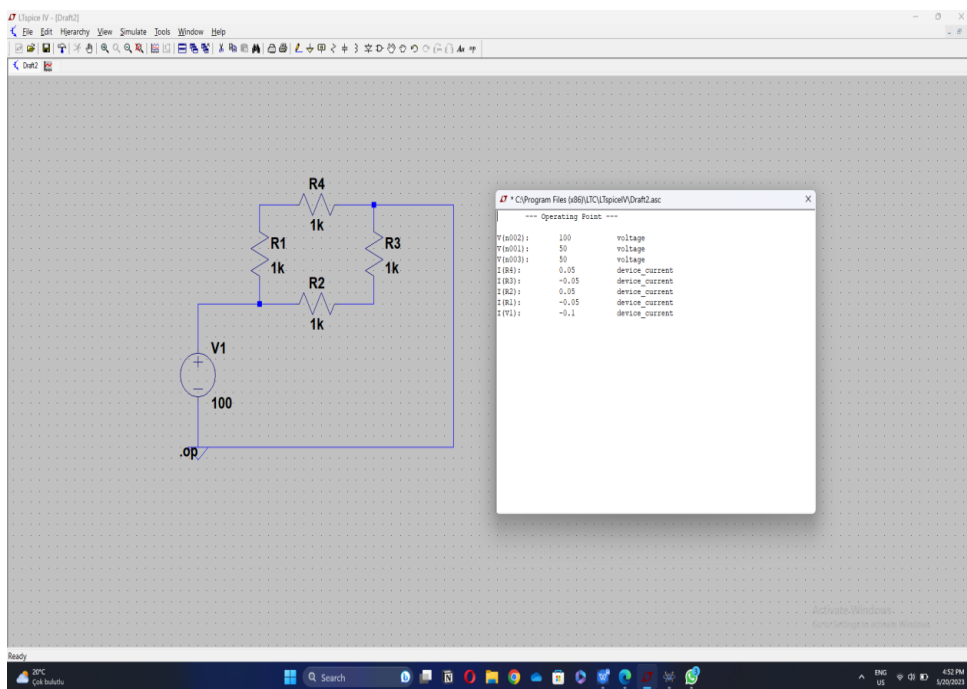


FIGURE 11

Let's explain what we've done. We have gathered the necessary materials to begin our project. With 30 resistors, a breadboard, and a multimeter in our school lab, we are ready to start building and testing circuits. The resistors will be used to regulate the flow of current through the circuit, while the breadboard provides a platform for us to easily connect and disconnect components as needed. The multimeter will be essential in measuring voltage, current, and resistance throughout our project. With these tools in hand, we can confidently start on our project to create an efficient and functional circuit with a 4 node resistor. We must carefully consider the placement of each resistor and ensure that they are connected properly to avoid any malfunctions or damage. Once we have successfully built our circuit, we can use the multimeter to test its performance and make any necessary adjustments. With patience and attention to detail, we can create a successful electrical project using these materials. We struggled for a while before figuring out how to connect the resistors to the breadboard in parallel and in series. We shortened the resistor legs to make it more stable and visible. Whether in series or parallel, we connected the resistors where they should have been. After we checked and made sure that every resistor was placed correctly, we measured the resistors using a multimeter. We plugged each probe of the multimeter in the opposite way, as shown in the figure. The multimeter showed a resistance of $0.998\text{ k}\Omega$. As previously mentioned, the resistance was $1\text{k}\Omega$ when simulating the four-node circuit, which had identical resistors connected in both series and parallel. The error percent between the theoretical part and the experimental part is 0.2%, which could have multiple reasons, such as the resistors, which could have an error percent, or the multimeter, which also has an error percent. . Another possible reason for the discrepancy could be the temperature of the circuit during the experiment, as temperature can affect resistance. It is also possible that there were slight variations in the connections or measurements taken during the experiment. However, despite this small error percent, the simulation and experiment still provide valuable insights into circuit behavior and can be used to make predictions for future circuits. Additionally, by comparing theoretical calculations with experimental results, engineers can identify areas where improvements can be made in their designs and increase overall efficiency. Overall, while there may be some discrepancies between theoretical calculations and experimental results, simulations and experiments remain essential tools for understanding and improving circuit design.

FOR 16 NODES

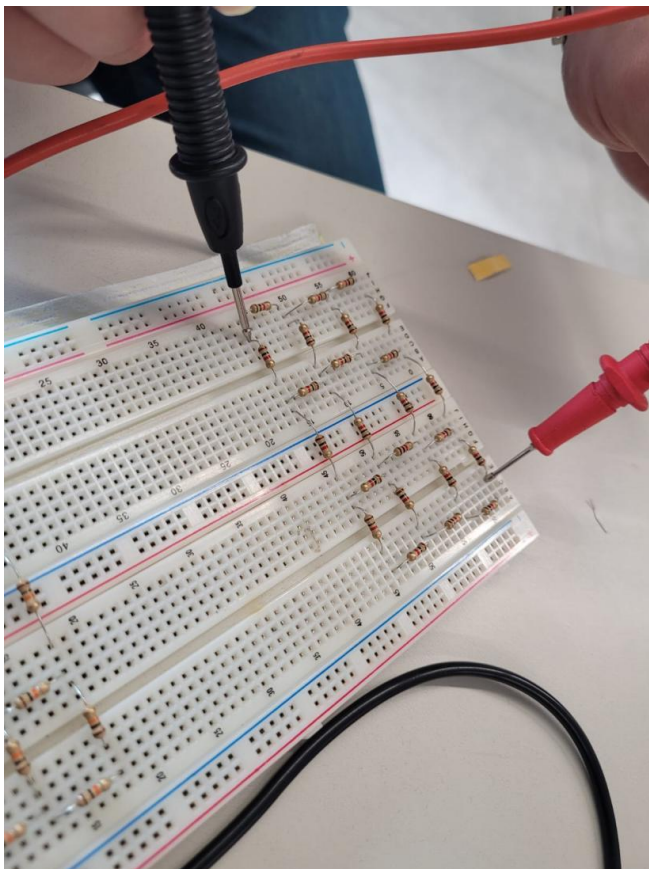


FIGURE 12

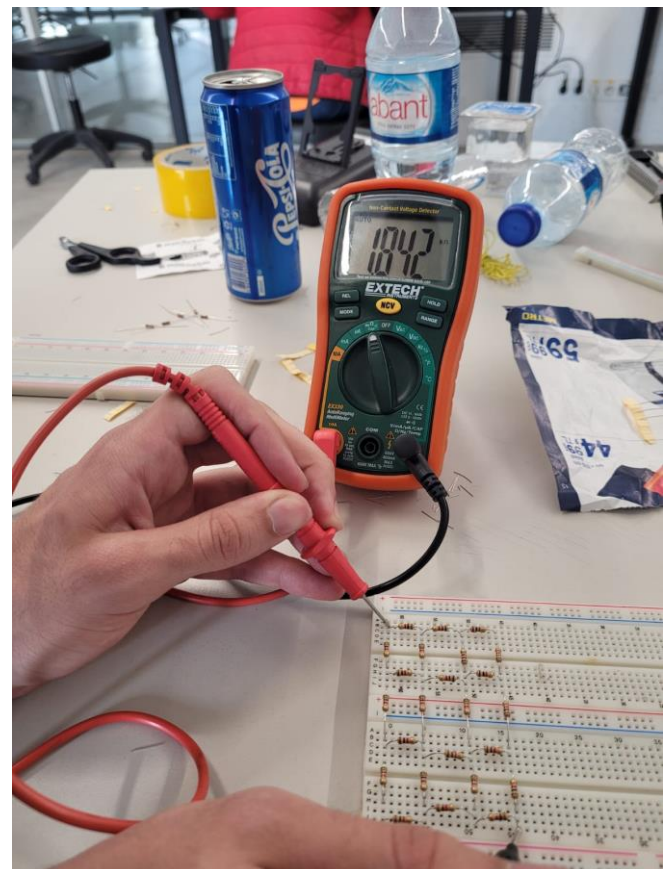


FIGURE 13

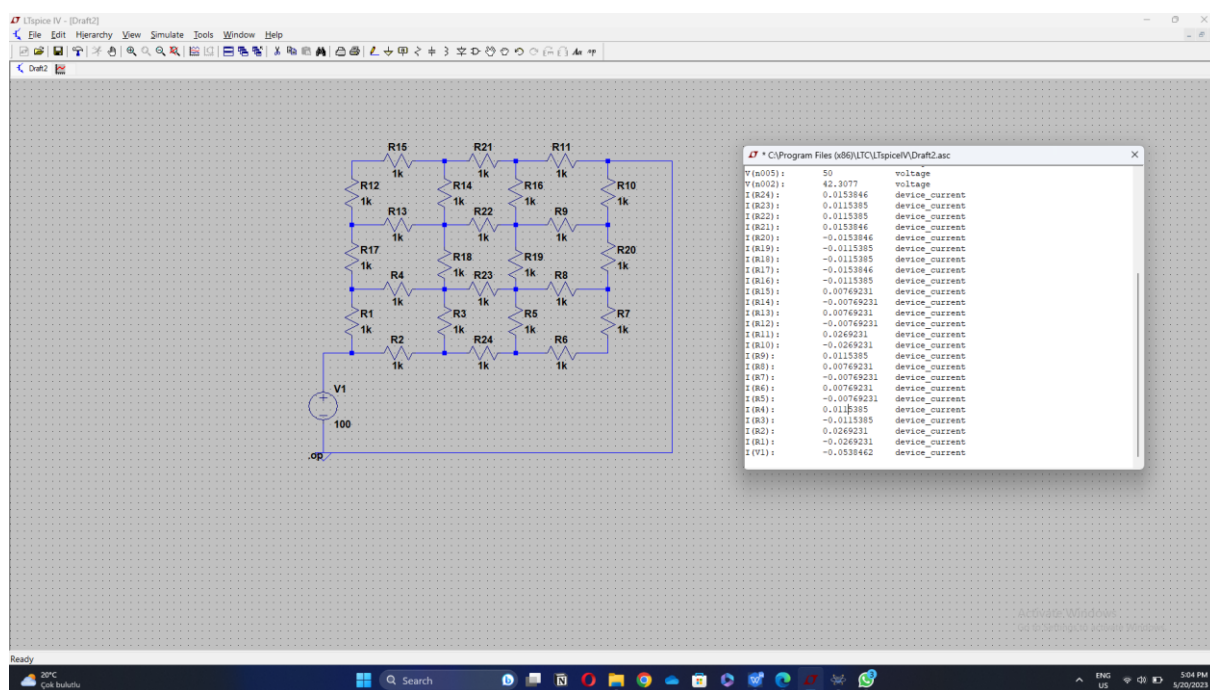


FIGURE 14

Our objective was to create an efficient and functional circuit with a 16-node resistor configuration. In order to accomplish this, we carefully considered where to place each resistor while ensuring proper connections to prevent any incorrect results or failures. Once the circuit was successfully assembled, we used the multimeter to evaluate its performance, making the necessary adjustments as required. With meticulous attention to detail, we confidently pursued our project by applying these materials.

Initially, we encountered difficulties in comprehending the appropriate methods of connecting the resistors in parallel and series configurations on the breadboard. However, through dedication, we overcame these obstacles and improved stability and visibility by shortening the resistor legs to make it more stable observable. Regardless of whether the resistors were connected in series or parallel, we ensured accurate placement.

Following the confirmation of proper resistor placement, we proceeded to measure the resistors' values using the multimeter. As shown in the figure, we inserted each multimeter probe in an opposite direction. The multimeter showed a resistance of 1.842k. When simulating the four-node circuit, which had identical resistors connected in both series and parallel, as was mentioned earlier, the resistance was 1.859k Ω . The error percent between the theoretical part and the experimental part is 0.9% er, which could have multiple reasons.

This variation could result from various factors, including the error percentage of the resistors and the multimeter's potential margin of error. Overall, we were able to successfully overcome the obstacles we faced and accurately measure the resistance of the resistors in both series and parallel connections. The slight discrepancy between the theoretical and experimental values could be attributed to various factors, but our dedication and attention to detail ensured that we achieved reliable results.

A capacitor network with 4, 16, 64, 128 and 256 nodes are created using a simulation tool and its equivalent capacitance is calculated.

The general formula used is as follows:

$$V_c = V_s + (V_0 - V_s)e^{\frac{-t}{\tau}} \quad \text{since } V_0 \text{ is } 0 \rightarrow V_s(1 - e^{\frac{-t}{\tau}}) \quad \tau = RC$$

$$1 - \frac{V_c}{V_s} = e^{\frac{-t}{\tau}} \rightarrow \ln\left(1 - \frac{V_c}{V_s}\right) = \frac{-t}{RC} \rightarrow Ceq = -\frac{t}{R} \ln\left(1 - \frac{V_c}{V_s}\right)$$

FOR 4 NODES

$$t = 4.38 \times 10^{-3} \text{ s}$$

$$R = 100 \text{ k}\Omega$$

$$V_c = 33.9 \text{ V}$$

$$V_s = 100 \text{ V}$$

$$\ln\left(1 - \frac{33.9}{100}\right) = \frac{-4.38 \times 10^{-3}}{100 \times C_{eq}} \quad C_{eq} = \frac{-4.38 \times 10^{-3}}{\ln\left(1 - \frac{33.9}{100}\right) \times 100} = 105.7 \times 10^{-6} F$$

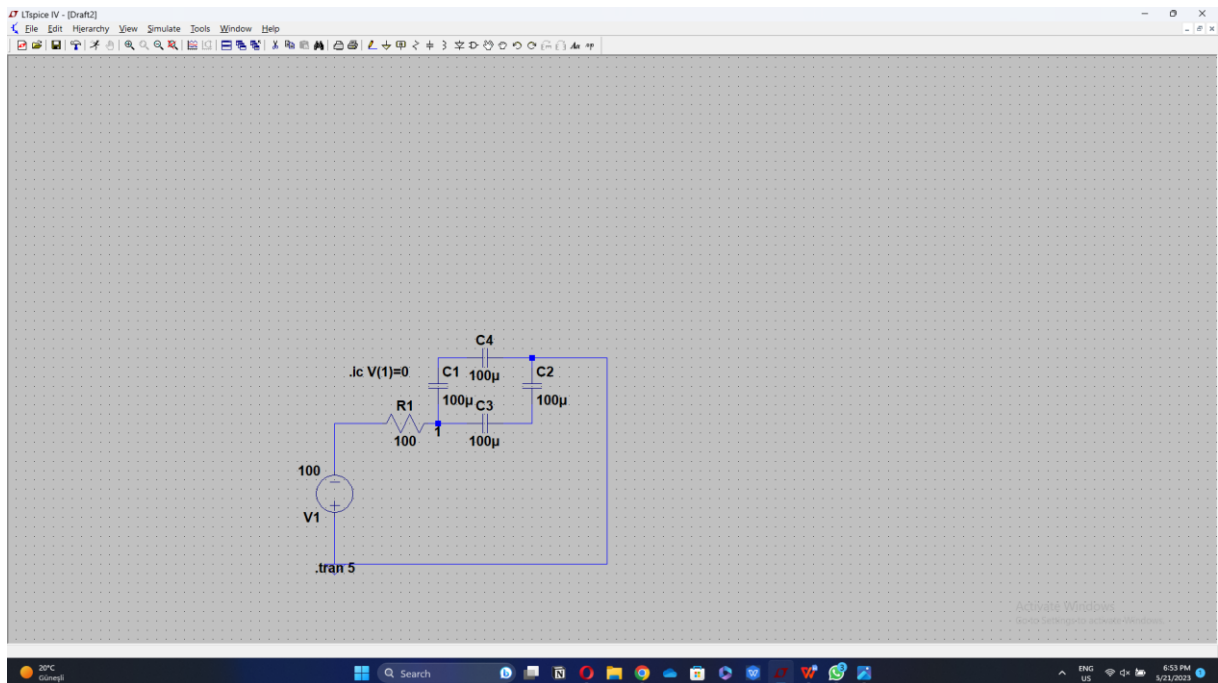


FIGURE 15

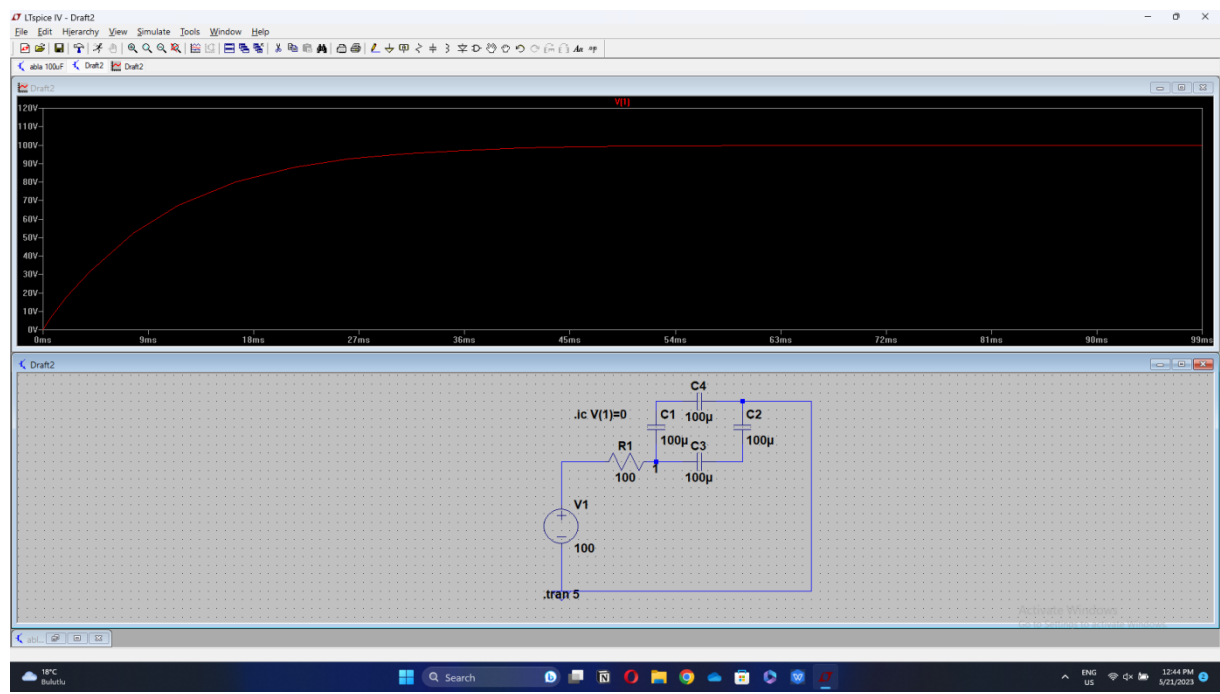


FIGURE 16

As shown in the Figure 16, the circuit's voltage increases in a parabolic curve way and ends up to 100 when capacitor start discharging. To calculate the equivalent capacitance of the 4 ,16 , 64 , 128 and 256 node circuit capacitors, we took a point from the graph as shown in the Figure 17 and by using the voltage and the time it occurred, we were able to determine the equivalent capacitance of 4 , 16 , 64 ,128 , and 256 node circuit capacitors as shown below.

That is, these graphs are drawn for each node value.

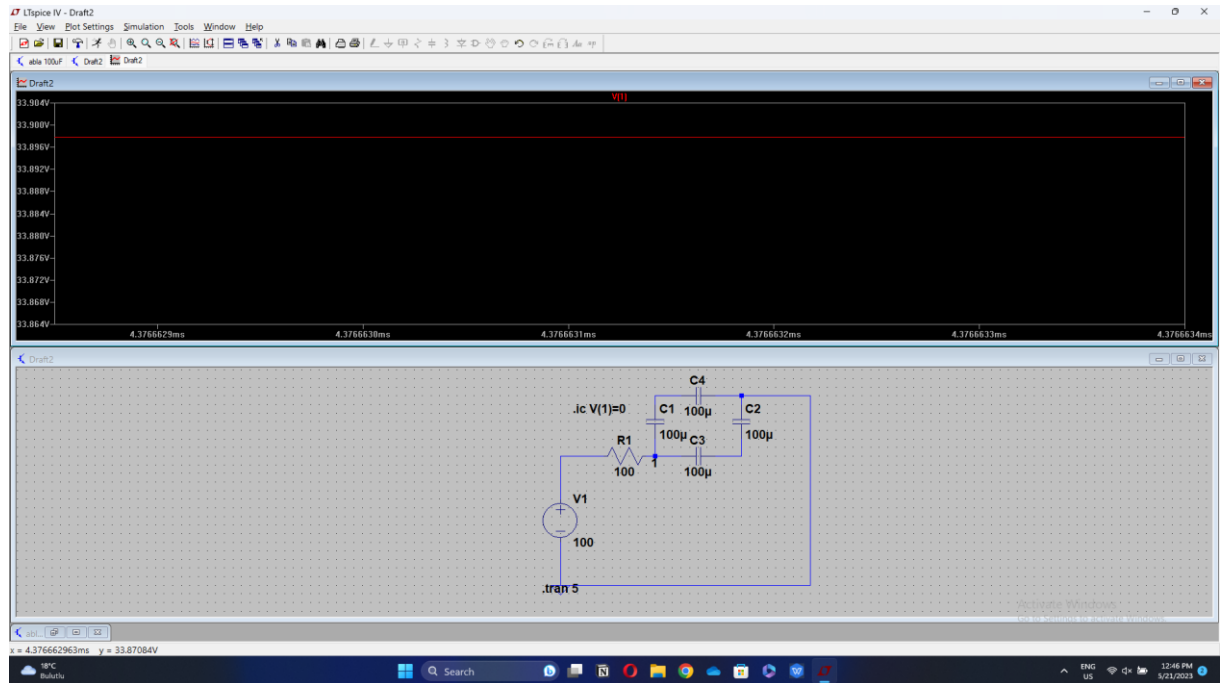


FIGURE 17

FOR 16 NODES

$$t = 3.11 \times 10^{-3} \text{ s}$$

$$R = 100 \text{ k}\Omega$$

$$V_c = 41.8 \text{ V}$$

$$V_s = 100 \text{ V}$$

$$C_{eq} = \frac{-3.11 \times 10^{-3}}{\ln\left(1 - \frac{41.8}{100}\right) \times 100} = 57.4 \times 10^{-6} \text{ F}$$

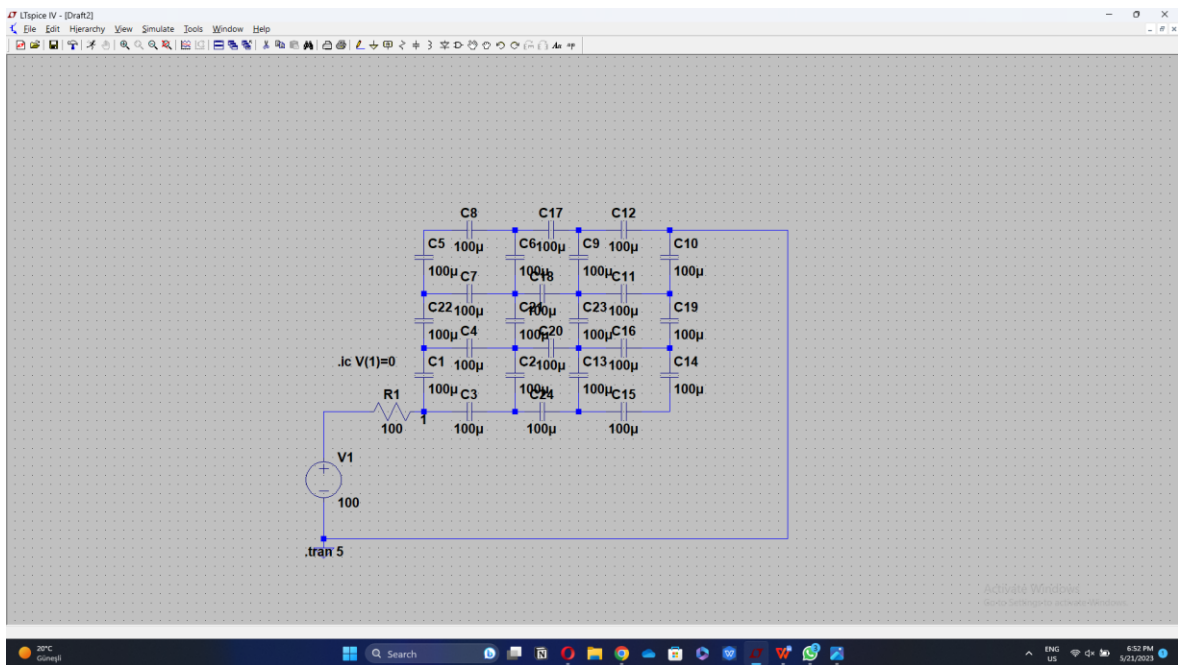


FIGURE 18

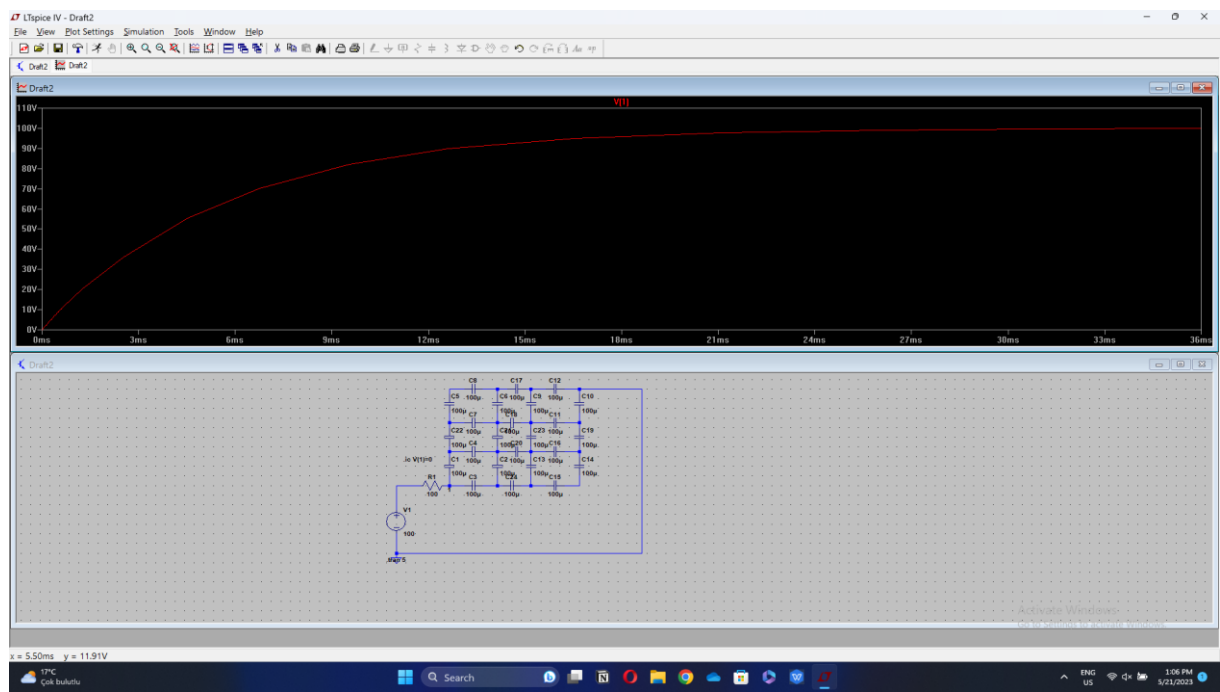


FIGURE 19

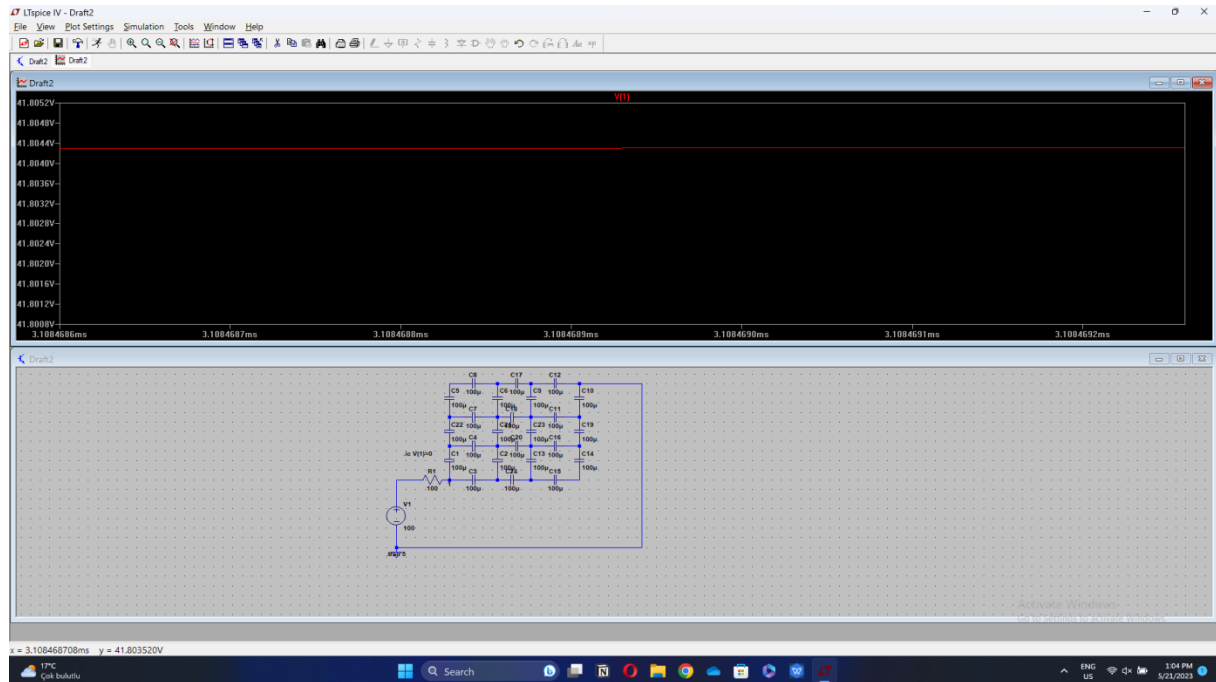


FIGURE 20

FOR 64 NODES

$$t = 8.99 \times 10^{-4} \text{ s}$$

$$R = 100 \text{k}\Omega$$

$$V_c = 21.2 \text{ V}$$

$$V_s = 100 \text{ V}$$

$$C_{eq} = \frac{-8.99 \times 10^{-4}}{\ln\left(1 - \frac{21.2}{100}\right) \times 100} = 37.7 \times 10^{-6} \text{ F}$$

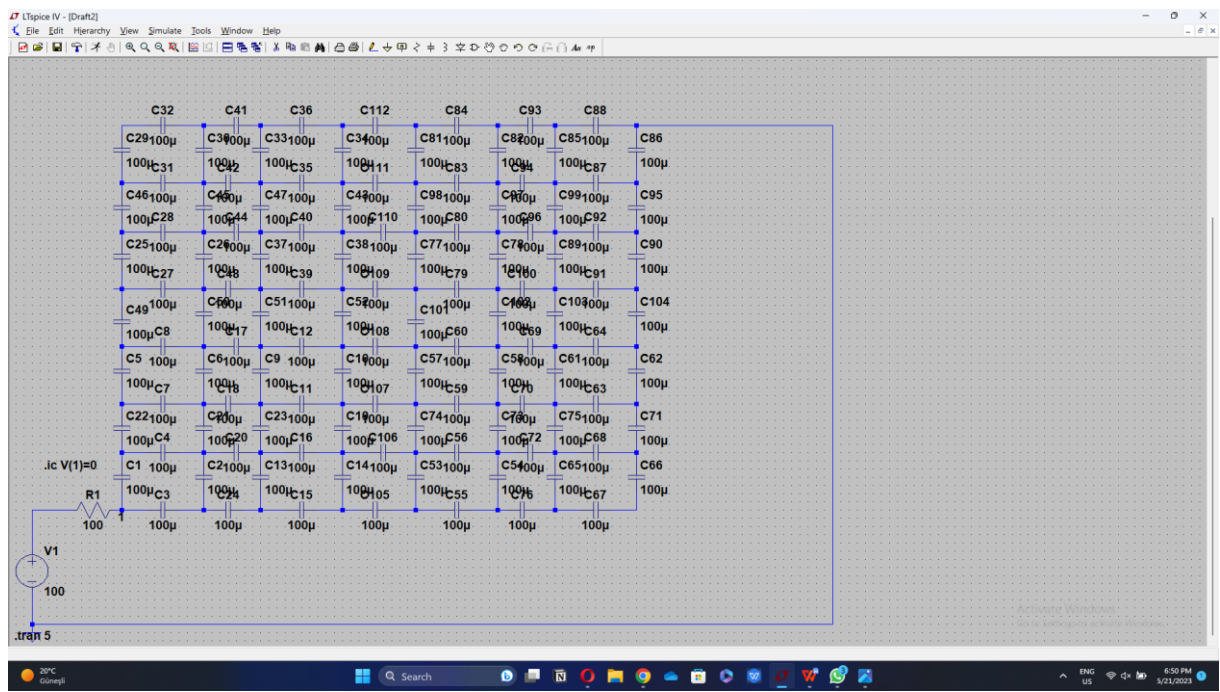


FIGURE 21

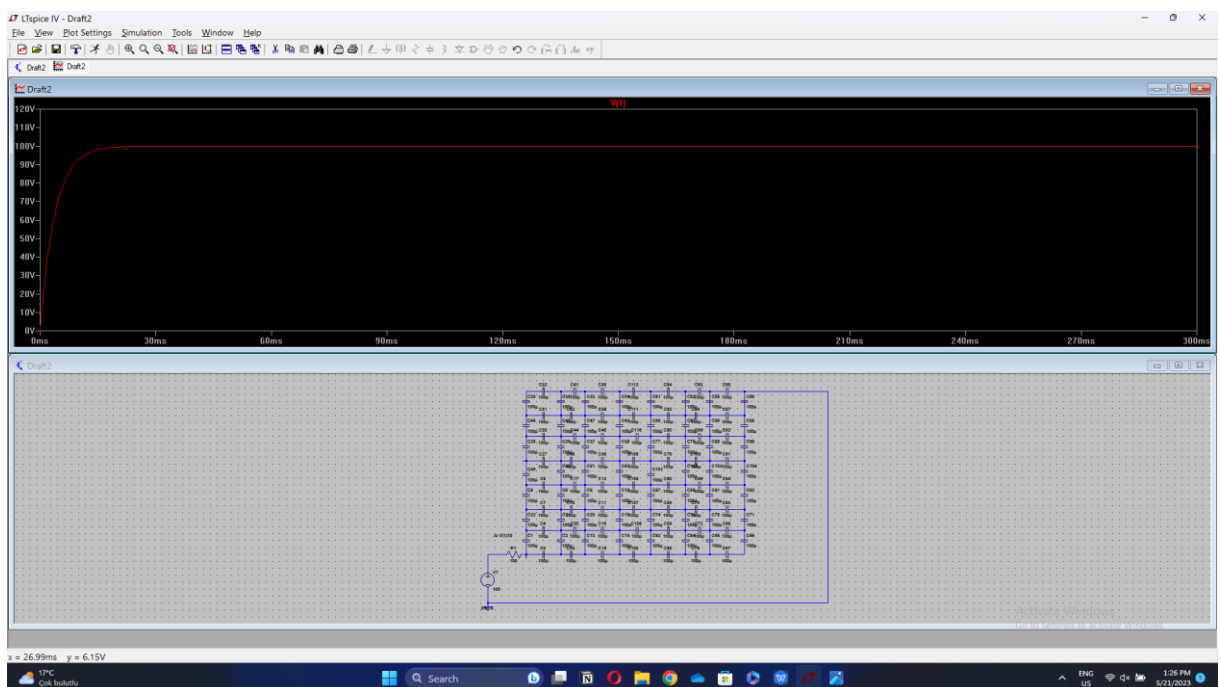


FIGURE 22

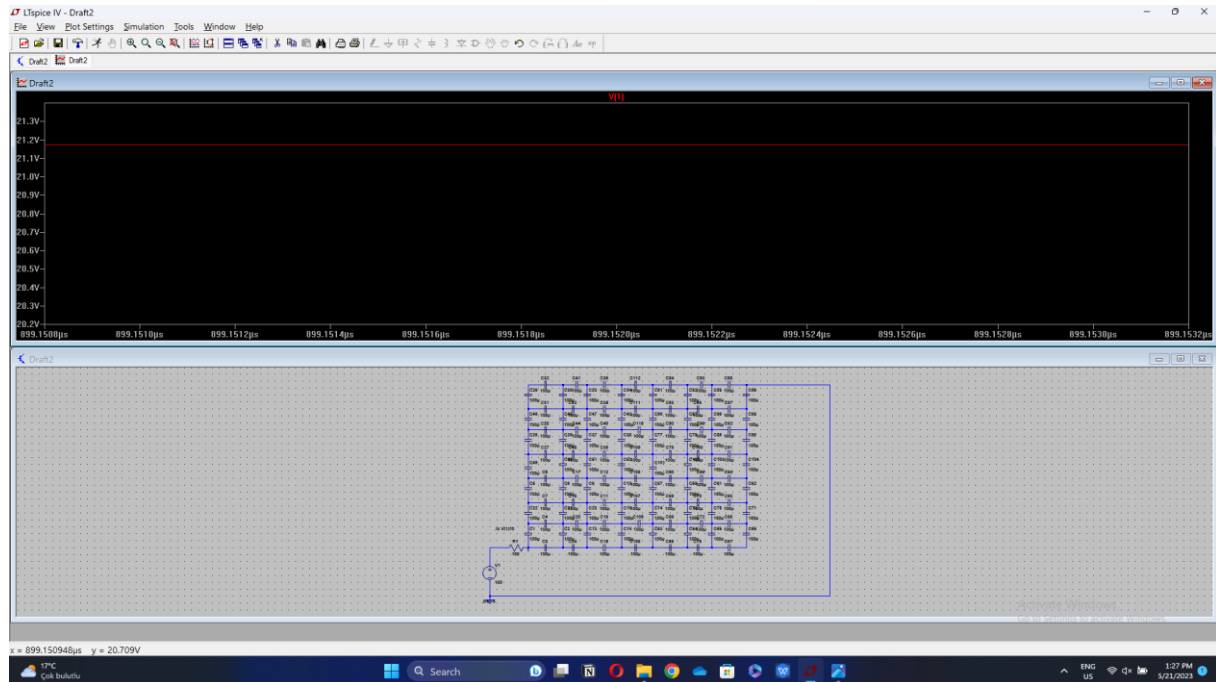


FIGURE 23

FOR 128 NODES

$$t = 1.90 \times 10^{-4} \text{ s}$$

$$R=100\text{k}\Omega$$

$$V_c = 6.60 \text{ V}$$

$$V_s = 100\text{V} \quad C_{eq} = \frac{-1.90 \times 10^{-4}}{\ln\left(1 - \frac{6.60}{100}\right) \times 100} = 27.8 \times 10^{-6} \text{ F}$$

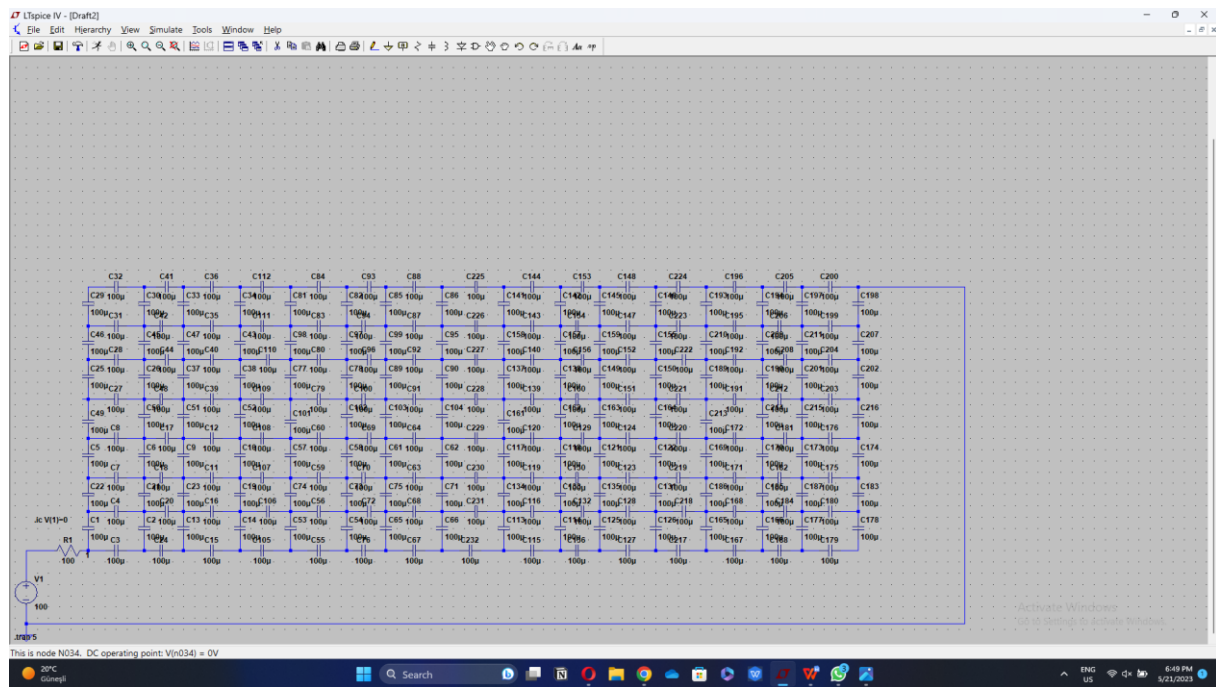


FIGURE 24

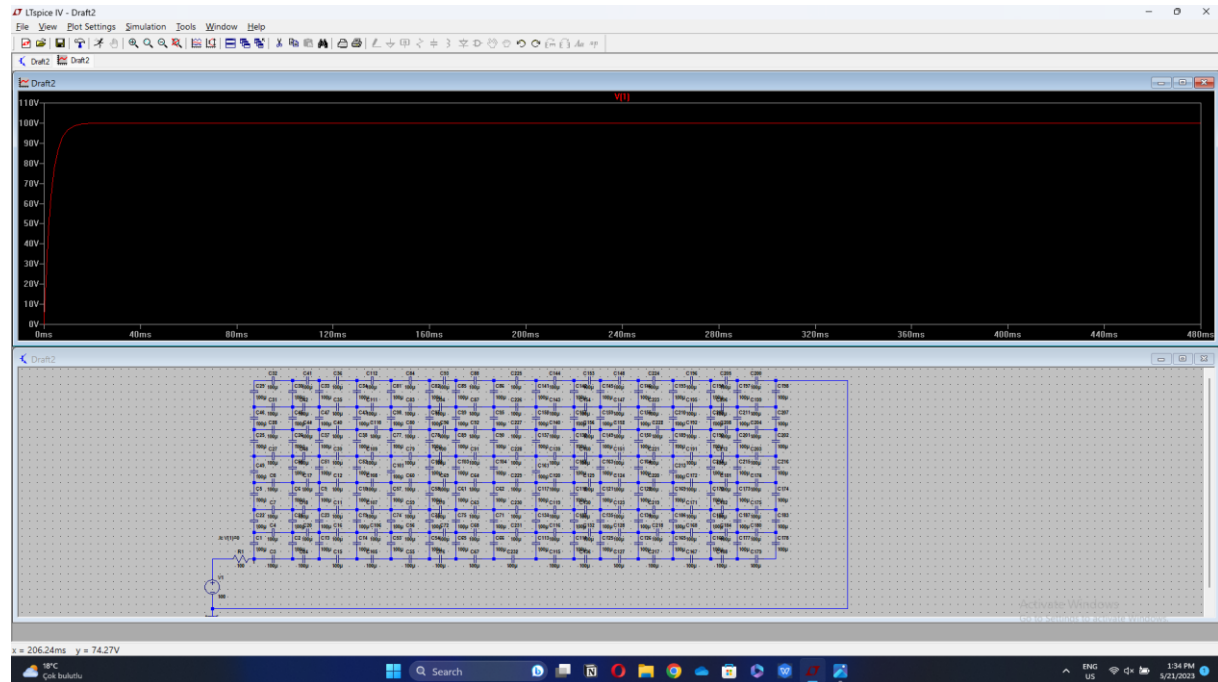


FIGURE 25

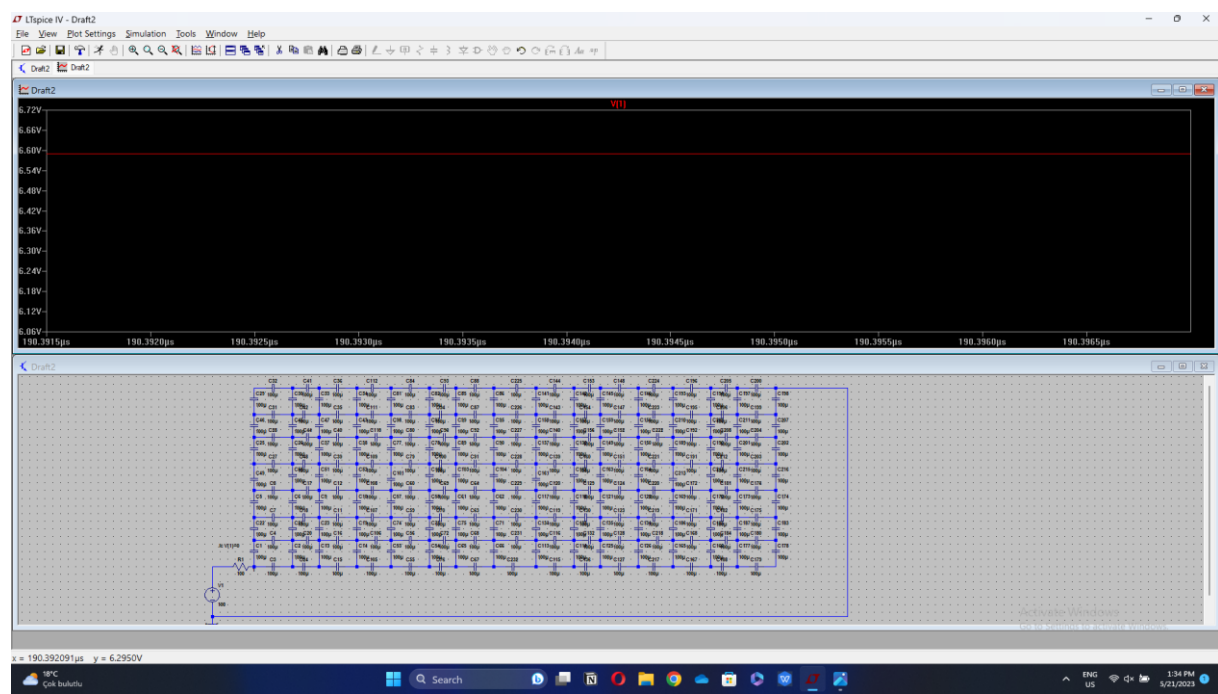


FIGURE 26

FOR 256 NODES

$$t = 1.89 \times 10^{-4} \text{ s}$$

$$R = 100 \text{ k}\Omega$$

$$V_c = 47.9 \text{ V}$$

$$V_s = 100 \text{ V}$$

$$C_{eq} = \frac{-1.89 \times 10^{-3}}{\ln\left(1 - \frac{47.9}{100}\right) \times 100} = 28.9 \times 10^{-6} \text{ F}$$

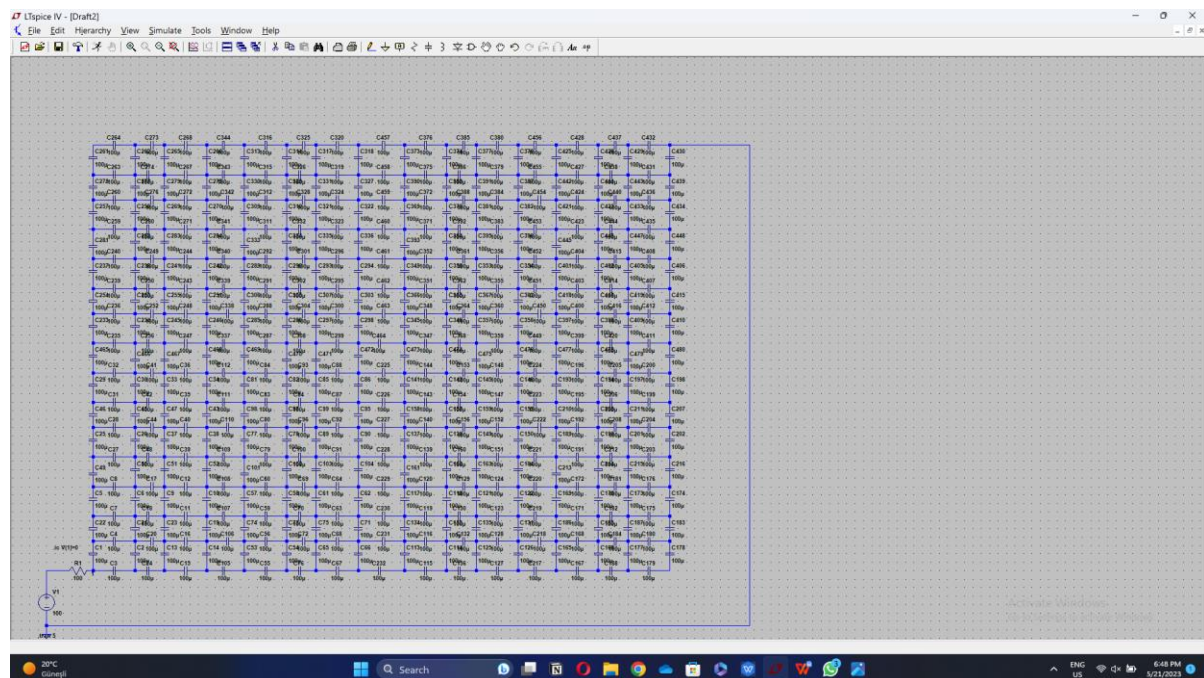


FIGURE 27

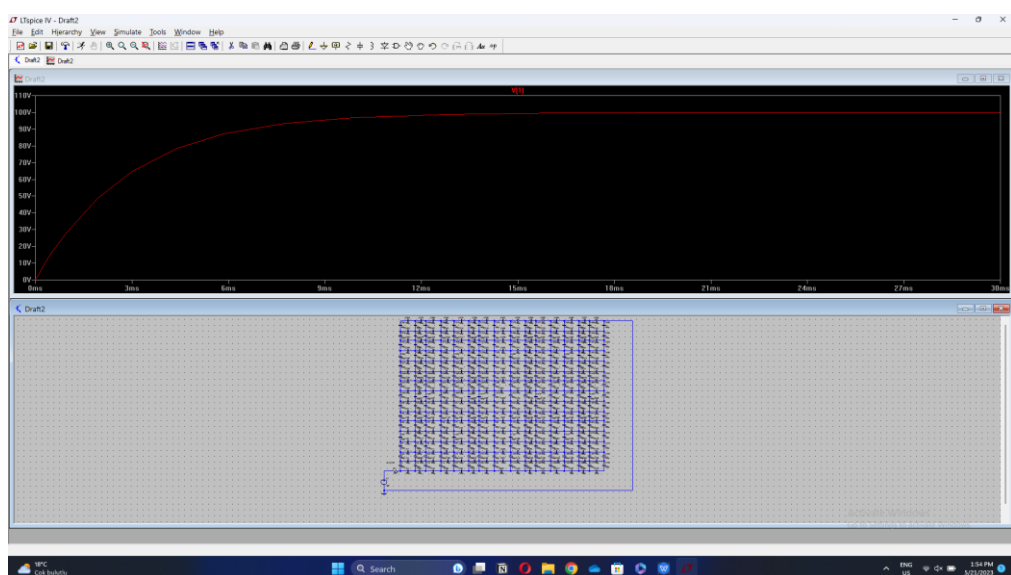


FIGURE 28

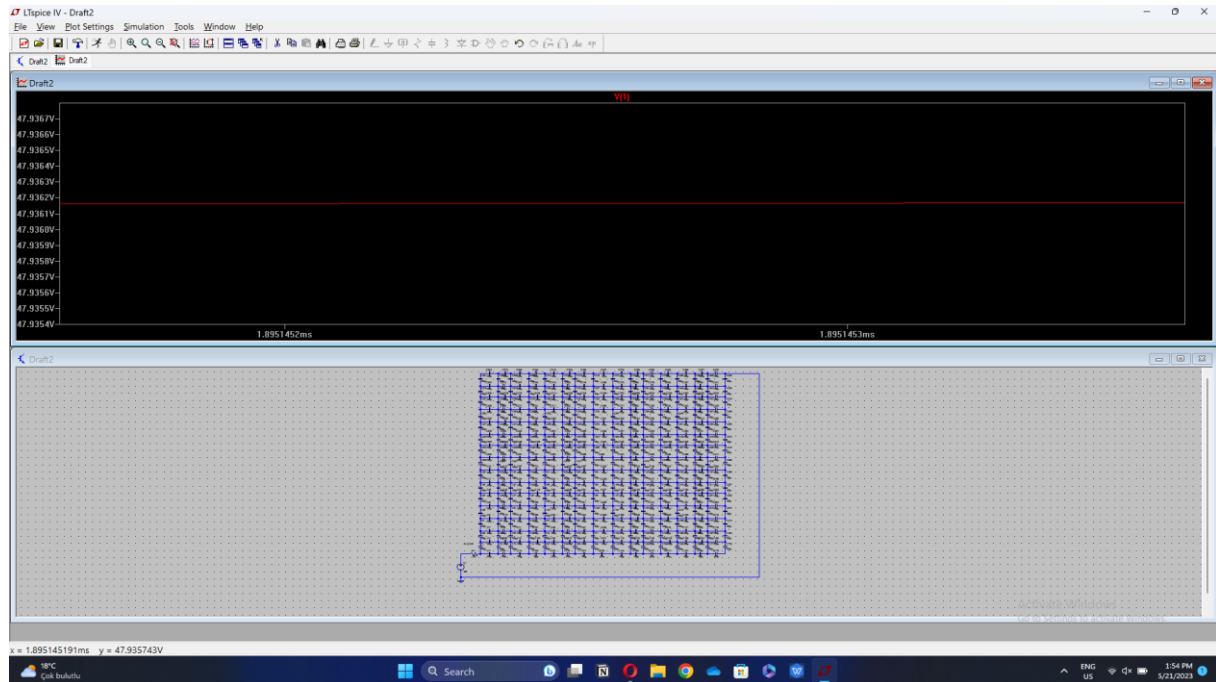


FIGURE 29

As the node count rises, the equivalent capacitance changes. The equivalent capacitance in 4 node capacitors was 105.7 microfarad. However, the equivalent capacitance in the 16 node capacitor was 57.4 microfarad. It showed a roughly 45.69% decrease between 4 and 16 nodes, which is a sizable drop. The equivalent capacitance in 64 node capacitors was 37.7 microfarad, not the same drop as the previous one. However, the equivalent capacitance in the 128 node capacitor was 27.8 microfarad, again indicating a smaller drop than the prior one. This leads us to the conclusion that as the drop percent varies frequently, the node's drop in capacitance decreases. The equivalent capacitance in the 256 node capacitor was 28.7 microfarad. The increase in 256 nodes demonstrates that the drop and increase can actually be affected by the number of nodes. This suggests that a node's capacitance is dynamic and changes depending on the voltage applied to it, rather than having a constant value. It is important to note that this phenomenon is not limited to the 256 node capacitor but can be observed in other larger node capacitors as well. Understanding this behavior is crucial for designing circuits that rely on stable capacitance values. In conclusion, the capacitance drop in node capacitors varies depending on the number of nodes and the voltage applied to them. This indicates that a node's capacitance is dynamic and not constant. This behavior must be taken into consideration when designing circuits that rely on stable capacitance values.

A capacitive network is created, consisting of 4 and 16 nodes, made of capacitors of our choice. A test method is developed to measure the equivalent capacitance:

FOR 4 NODES

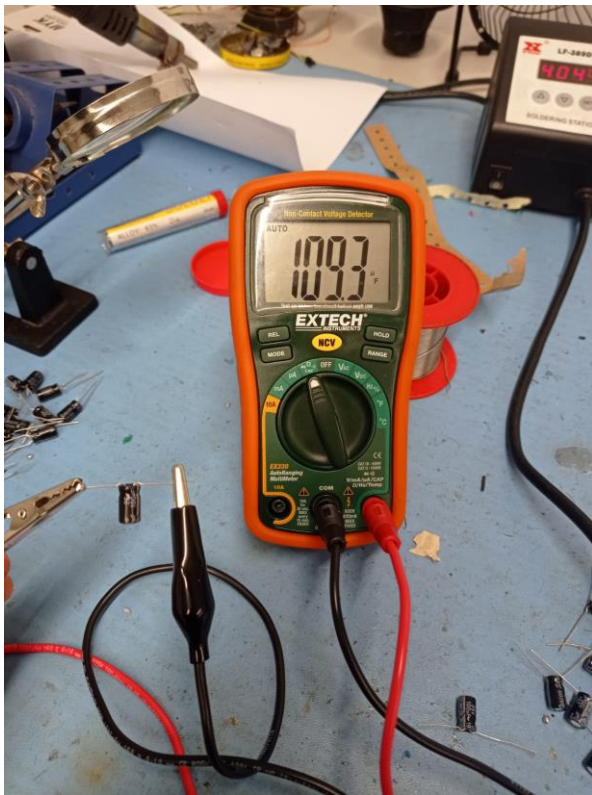


FIGURE 30

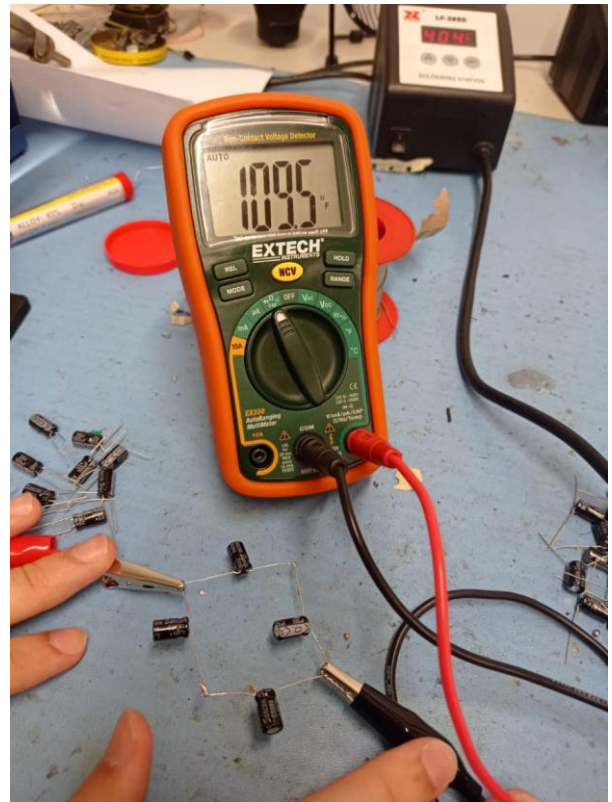


FIGURE 31

With the intention of building and testing the capacitance of a 4 node capacitor, we started our experiment in the school lab, where we had a soldering iron, solder wire , a multimeter, and four capacitors at our disposal. We connected the capacitors using solder and its wire in a 4 node circuit shape, as shown in the Figure 31. Then We began by measuring just one capacitor to determine the capacitors' total capacitance margin error. By following the prescribed figure, we correctly connected the multimeter probes in an opposing manner. As shown in the Figure 30 above , the capacitance was 109.3 Microfarad, which shows an error of 9.3% because it was shown in the capacitor that it was only 100 Microfarad. So, we can conclude that the 9.3% error is in fact the capacitors' error. We then proceeded to measure the capacitance of a 4 node capacitor circuit using the multimeter. Finally, we analyzed our results and compared them to theoretical calculations, finding that our experimental values were within a reasonable margin of error. The percent of error was 9.5%, which, as we stated earlier, was due to the capacitor margin error. Overall, this experiment provided us with valuable hands-on experience working with capacitors and testing their properties in a real-world setting. Through careful research and experimentation, we determined the appropriate method of connecting the capacitors using solder. To ensure stability and visual clarity, we made necessary adjustments, such as modifying the capacitor leads and ensuring that the solder wire connected the two or more capacitors with each other. As with the capacitor

simulation, any observed discrepancy between the theoretical and experimental values could be attributed to factors such as inherent capacitor tolerances or the multimeter's margin of error. Nevertheless, the insights gained from this simulation and experiment will contribute to our understanding of capacitor behavior and aid in the improvement of future circuit designs.

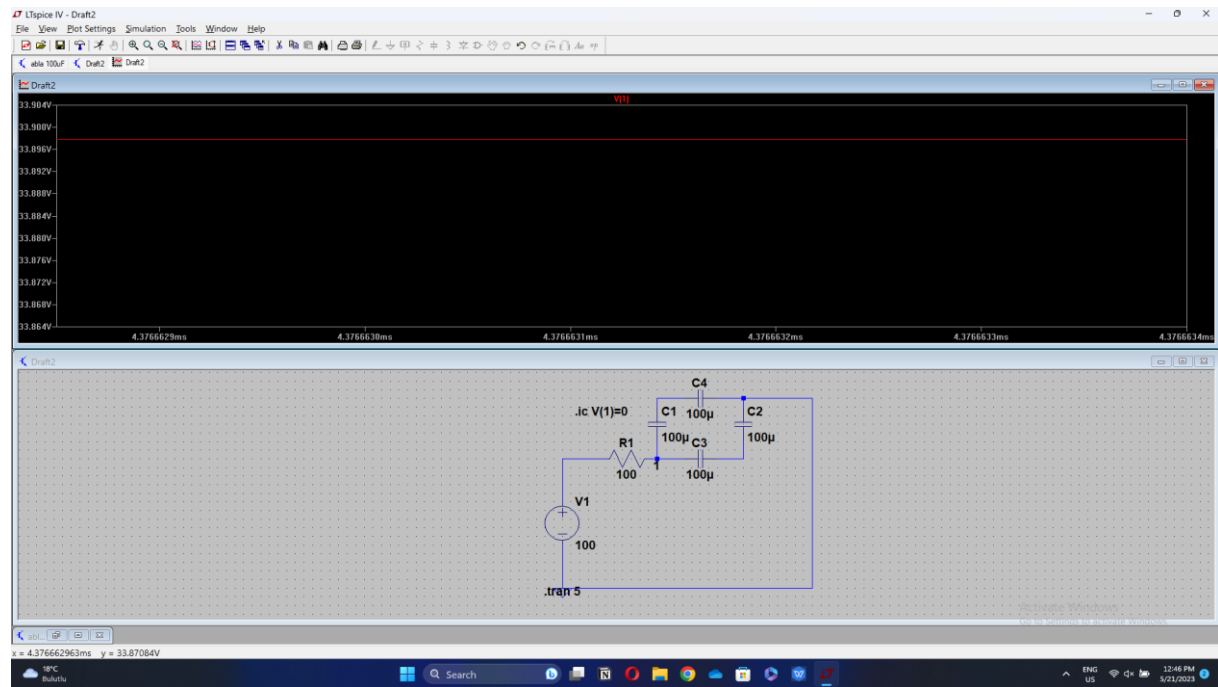


FIGURE 32

FOR 16 NODES

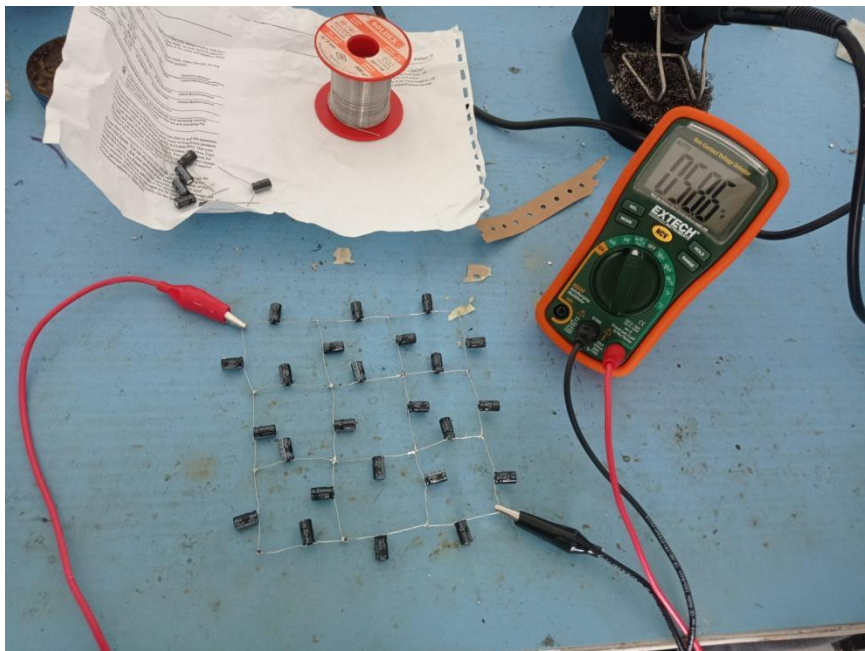


FIGURE 33

As shown in the figure 33 , by using the solder, which was in the school lab, we were able to connect the 24 capacitors in a 16 node circuit shape. We used the same materials as in the 4 node capacitor, which are a soldering iron, solder wire , a multimeter, and 24 capacitors at our disposal. As shown in the figure , the equivalent capacitance of the 16 node circuit appeared to be 58.6 microfarads. As we showed earlier , the simulation's result of the 16 node capacitors was 57.4 micro, which shows that the error percent was 2.1%. This was determined by using the voltage circuit's graph and using the formula for equivalent capacitance, which was used in the earlier part. By choosing one value from the graph of the voltage and knowing its time from the graph, we were able to use the equation that we used earlier to determine the theoretical equivalent capacitance of the 16 node capacitor. This process of determining the equivalent capacitance is crucial in designing circuits as it allows us to simplify complex circuits into a single equivalent capacitor. The results were within our expected range, indicating that the circuit was functioning properly. However, we noticed some fluctuations in the readings, which we attributed to stray capacitance and, as we stated earlier, the capacitance margin error, which is 9.3%. Overall, this project taught us valuable skills in circuit design and troubleshooting, and we are excited to apply these skills to future projects.

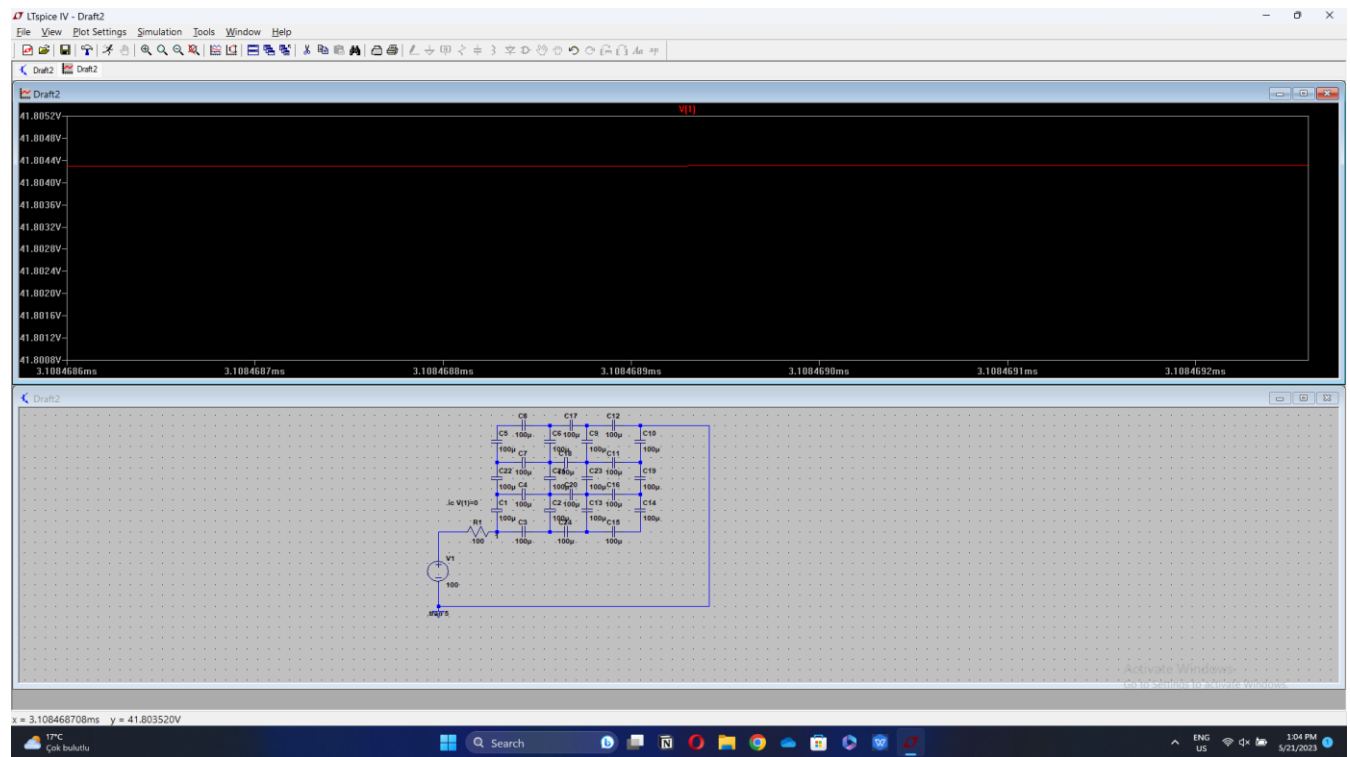


FIGURE 34

Part 2

When considering a pair of inert gas atoms, labeled as atom 1 and atom 2, that are separated by a distance r , the interaction between them can be described using a model involving the coupling of two dipoles. The first dipole arises from a temporary fluctuation in the electron distribution of atom 1. This fluctuation induces an electric field, which in turn induces a dipole moment in atom 2. The interaction between these two induced dipoles gives rise to an attractive force between the atoms, known as the van der Waals force. This force is responsible for the non-covalent attraction between neutral atoms and molecules and plays a significant role in determining the stability and behavior of substances at the molecular level. When it is written as potential energy, it is called Lennard-Jones potential and its equations is as follows:

$$U(r) = 4\epsilon \left[\left(\frac{\sigma}{r} \right)^{12} - \left(\frac{\sigma}{r} \right)^6 \right]$$

To find the force for the electrostatic potential energy as a function of distance (r), the following steps are done.

The relationship between force and energy is:

$$F(r) = \frac{-dU}{dr}$$

The result is obtained when the derivative of the potential energy with respect to r is taken.

$$\begin{aligned} F(r) &= -4\epsilon \left[\left(\frac{-12\sigma^{12}}{r^{13}} \right) - \left(\frac{-6\sigma^6}{r^7} \right) \right] \\ F(r) &= \frac{48\epsilon\sigma^{12}}{r^{13}} - \frac{24\epsilon\sigma^6}{r^7} \end{aligned}$$

To investigate the extreme (minimum and maximum) properties for $U(r)$ and $F(r)$ functions, the derivatives of both equations are taken and set to zero. So,

$$\begin{aligned} U'(r) &= \frac{dU}{dr} = 0 \\ \frac{dU}{dr} &= 4\epsilon \left[\left(\frac{-12\sigma^{12}}{r^{13}} \right) - \left(\frac{-6\sigma^6}{r^7} \right) \right] \\ U'(r) &= 24\epsilon \left(\frac{\sigma^6}{r^7} - \frac{2\sigma^{12}}{r^{13}} \right) = 0 \\ r &= \sqrt[6]{2}\sigma = 1.225\sigma \end{aligned}$$

When the r value found is substituted in the $U(r)$ equation, the result is $-\epsilon$. ϵ is a positive number. So, this r value is the absolute minimum point and there isn't maximum point for $U(r)$ equation.

$$F'(r) = \frac{dF}{dr} = 0$$

$$F(r) = \frac{48\epsilon\sigma^{12}}{r^{13}} - \frac{24\epsilon\sigma^6}{r^7}$$

$$F(r) = 24\epsilon \left(\frac{2\sigma^{12}}{r^{13}} - \frac{\sigma^6}{r^7} \right)$$

$$F'(r) = 24\epsilon \left(\frac{7\sigma^6}{r^8} - \frac{26\sigma^{12}}{r^{14}} \right) = 0$$

$$r = \sqrt[6]{\frac{26}{7}\sigma} = 1.2445\sigma$$

So, this r value is the minimum point of F(r) function and there is not maximum point.

When the graphs of these two functions are drawn in MATLAB, the following graph in Figure 35 is obtained.

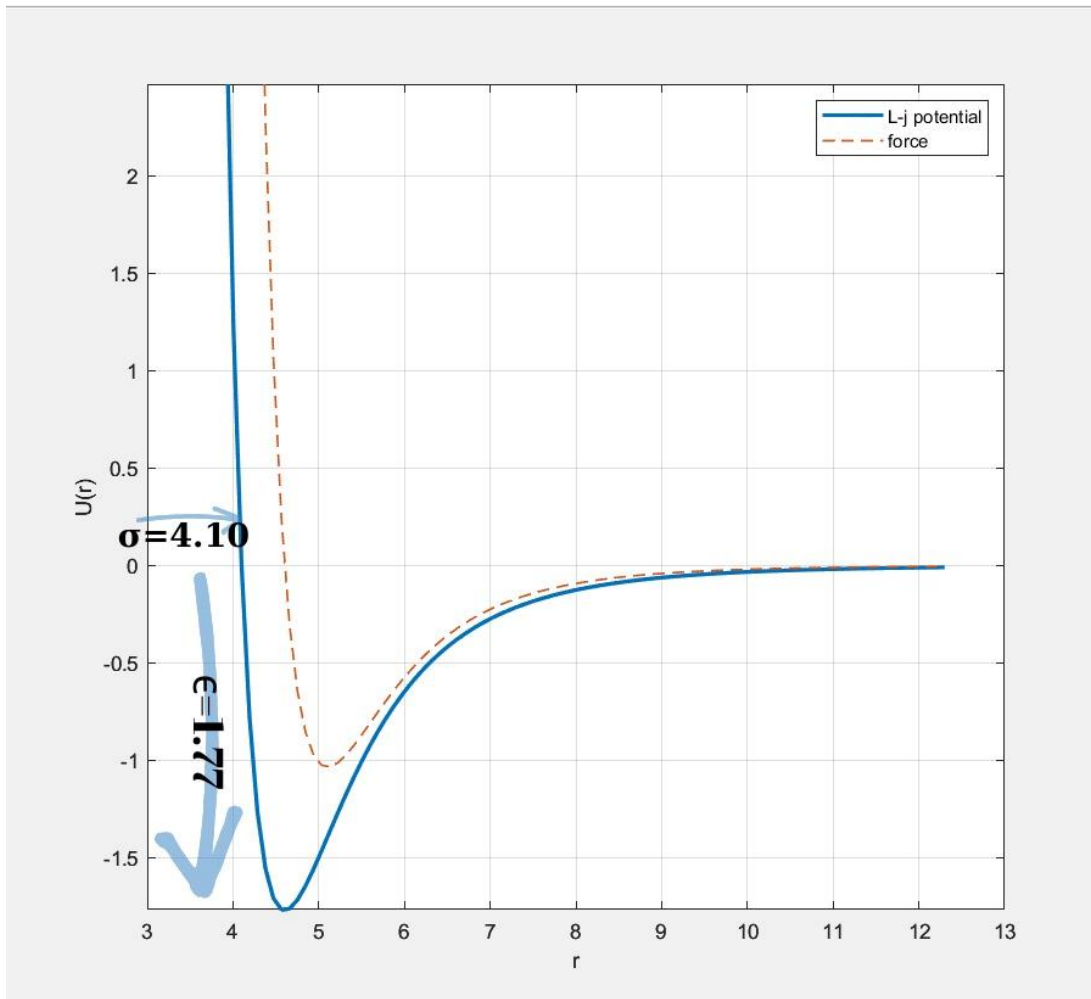


FIGURE 35

This graph is drawn based on the potential of between two Xe atoms. The ε value is 1.77 kJ/mol and the σ value is 4.10 Angstroms for Xenon.

Figure 36 shows the general graph of the Lennard Jones potential. When we compare Figure 35 and Figure 36, it is proved that the minimum value of r is $-\varepsilon$. This minimum represents the equilibrium distance at which the attractive and repulsive forces between the atoms balance out.

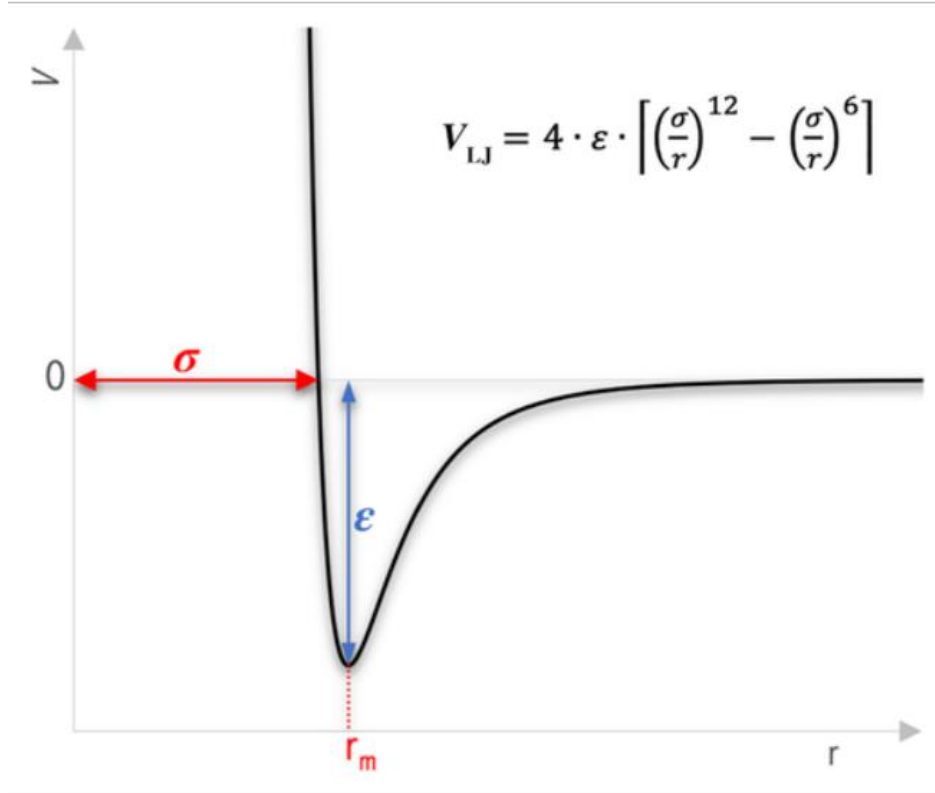


FIGURE 36

ε represents the depth of the well and indicates the strength of the attractive force between the two particles.

σ denotes the point at which the intermolecular potential between the two particles becomes zero. It provides a measurement of the minimum proximity achievable between two nonbonding particles and is commonly known as the van der Waals radius.

r is the separation distance between both particles, measured from the center of one particle to the center of the other particle.

The equilibrium distance, denoted by r_{eq} , is the distance at which the potential energy is at a minimum. In other words, it is the distance where the attractive and repulsive forces between the two particles balance out. To find r_{eq} for the Lennard-Jones potential, we need to minimize the potential energy with respect to r .

$$\frac{dU}{dr} = 4\epsilon \left[\left(\frac{-12\sigma^{12}}{r^{13}} \right) - \left(\frac{-6\sigma^6}{r^7} \right) \right]$$

$$U'(r) = 24\epsilon \left(\frac{\sigma^6}{r^7} - \frac{2\sigma^{12}}{r^{13}} \right) = 0$$

$$r_{eq} = \sqrt[6]{2}\sigma = 1.225\sigma$$

Taking into account the spherical symmetry of the force with respect to the radial measure r , the following operations are performed to write the equation of the force F components F_x , F_y , F_z in Cartesian coordinates.

$$x = r \cdot \sin\theta \cdot \cos\phi$$

$$y = r \cdot \sin\theta \cdot \sin\phi$$

$$z = r \cdot \cos\theta$$

$$x^2 + y^2 = (r \cdot \sin\theta \cdot \cos\phi)^2 + (r \cdot \sin\theta \cdot \sin\phi)^2$$

$$x^2 + y^2 = r^2 \cdot (\sin\theta)^2 \cdot (\cos^2\phi + \sin^2\phi)$$

$$(\cos^2\phi + \sin^2\phi) = 1$$

$$x^2 + y^2 = r^2 \cdot \sin^2\theta$$

$$x^2 + y^2 + z^2 = r^2 \cdot \sin^2\theta + r^2 \cdot \cos^2\theta$$

$$x^2 + y^2 + z^2 = r^2 (\sin^2\theta + \cos^2\theta)$$

$$(\sin^2\theta + \cos^2\theta) = 1$$

$$x^2 + y^2 + z^2 = r^2$$

$$r = \sqrt{x^2 + y^2 + z^2}$$

$$\hat{r} = \frac{\hat{x} \cdot x}{\sqrt{x^2 + y^2 + z^2}} + \frac{\hat{y} \cdot y}{\sqrt{x^2 + y^2 + z^2}} + \frac{\hat{z} \cdot z}{\sqrt{x^2 + y^2 + z^2}}$$

$$\vec{F}_x = \frac{-\hat{x} \cdot x}{\sqrt{x^2 + y^2 + z^2}} \left(\frac{dU(r)}{dr} \right) \Big|_{r=\sqrt{x^2+y^2+z^2}}$$

$$\vec{F}_x = \frac{\hat{x} \cdot x}{\sqrt{x^2 + y^2 + z^2}} 24\epsilon \left[\frac{2\sigma^{12}}{(\sqrt{x^2 + y^2 + z^2})^{13}} - \frac{\sigma^6}{(\sqrt{x^2 + y^2 + z^2})^7} \right]$$

$$\vec{Fy} = \frac{-\hat{\mathbf{y}} \cdot \mathbf{y}}{\sqrt{x^2 + y^2 + z^2}} \left(\frac{dU(r)}{dr} \right) \Big|_{r=\sqrt{x^2+y^2+z^2}}$$

$$\vec{Fy} = \frac{\hat{\mathbf{y}} \cdot \mathbf{y}}{\sqrt{x^2 + y^2 + z^2}} 24\epsilon \left[\frac{2\sigma^{12}}{(\sqrt{x^2 + y^2 + z^2})^{13}} - \frac{\sigma^6}{(\sqrt{x^2 + y^2 + z^2})^7} \right]$$

$$\vec{Fz} = \frac{-\hat{\mathbf{z}} \cdot \mathbf{z}}{\sqrt{x^2 + y^2 + z^2}} \left(\frac{dU(r)}{dr} \right) \Big|_{r=\sqrt{x^2+y^2+z^2}}$$

$$\vec{Fz} = \frac{\hat{\mathbf{z}} \cdot \mathbf{z}}{\sqrt{x^2 + y^2 + z^2}} 24\epsilon \left[\frac{2\sigma^{12}}{(\sqrt{x^2 + y^2 + z^2})^{13}} - \frac{\sigma^6}{(\sqrt{x^2 + y^2 + z^2})^7} \right]$$

$$\begin{aligned}\vec{F} &= -\frac{\hat{\mathbf{x}} \cdot \mathbf{x} + \hat{\mathbf{y}} \cdot \mathbf{y} + \hat{\mathbf{z}} \cdot \mathbf{z}}{\sqrt{x^2 + y^2 + z^2}} \left(\frac{dU(r)}{dr} \right) \Big|_{r=\sqrt{x^2+y^2+z^2}} \\ \vec{F} &= \frac{\hat{\mathbf{x}} \cdot \mathbf{x} + \hat{\mathbf{y}} \cdot \mathbf{y} + \hat{\mathbf{z}} \cdot \mathbf{z}}{\sqrt{x^2 + y^2 + z^2}} 24\epsilon \left[\frac{2\sigma^{12}}{\sqrt{x^2 + y^2 + z^2}} - \frac{\sigma^6}{\sqrt{x^2 + y^2 + z^2}} \right]\end{aligned}$$

To find the Cartesian components of the gradient vector for $U(r)$, the following operations are made:

$$\begin{aligned}U(x, y, z) &= 4\epsilon \left[\left(\frac{\sigma}{\sqrt{x^2 + y^2 + z^2}} \right)^{12} - \left(\frac{\sigma}{\sqrt{x^2 + y^2 + z^2}} \right)^6 \right] \\ \nabla U &= \frac{\partial U}{\partial x} \hat{\mathbf{i}} + \frac{\partial U}{\partial y} \hat{\mathbf{j}} + \frac{\partial U}{\partial z} \hat{\mathbf{k}} \\ \nabla U &= 4\epsilon \left[\left(\frac{-12\sigma^{12}x}{(x^2 + y^2 + z^2)^7} \right) - \left(\frac{-8\sigma^6x}{(x^2 + y^2 + z^2)^7} \right) \right] \hat{\mathbf{i}} + \\ &\quad 4\epsilon \left[\left(\frac{-12\sigma^{12}y}{(x^2 + y^2 + z^2)^7} \right) - \left(\frac{-8\sigma^6y}{(x^2 + y^2 + z^2)^7} \right) \right] \hat{\mathbf{j}} + \\ &\quad 4\epsilon \left[\left(\frac{-12\sigma^{12}z}{(x^2 + y^2 + z^2)^7} \right) - \left(\frac{-8\sigma^6z}{(x^2 + y^2 + z^2)^7} \right) \right] \hat{\mathbf{k}}\end{aligned}$$

The relationship between work and energy is utilized when finding the work W done by the Lennard-Jones force to transfer the electric charge e from the initial position $r = \sigma$ to infinity.

$$W = \int_{\sigma}^{\infty} \overrightarrow{F(r)} \cdot d\overrightarrow{r}$$

$$W = \int_{\sigma}^{\infty} 24\epsilon \left(\frac{2\sigma^{12}}{r^{13}} - \frac{\sigma^6}{r^7} \right) dr$$

$$W = 4\epsilon \left[\left(\frac{\sigma}{\infty} \right)^6 - \left(\frac{\sigma}{\infty} \right)^{12} \right] - 4\epsilon \left[\left(\frac{\sigma}{\sigma} \right)^6 - \left(\frac{\sigma}{\sigma} \right)^{12} \right] = 0$$

Therefore, the result of the work done is found as 0.

Part 3

Figure 37 shows the simple "toy" model, which strangely reflects the process of interaction of electrons in a metal with the oscillating ions of the crystal lattice. In this model, the white ball represents the electron and the direction of motion is indicated by the arrow. In the corridor are lattice ions making oscillating motions lined up with arrows. These lattice ions are represented by black balls. It will be shown how this model reflects the resistance to the movement of electrons under the influence of an external electric field, or in other words, the resistance to the flow of electric current through a metal. The electrical resistance of the moving electrons is due to the thermal vibrations of the ions in the crystal lattice. Therefore, the white ball schematically reflects the motion of an electron under the influence of an electric field, and the black balls represent metal ions released due to thermal vibrations.

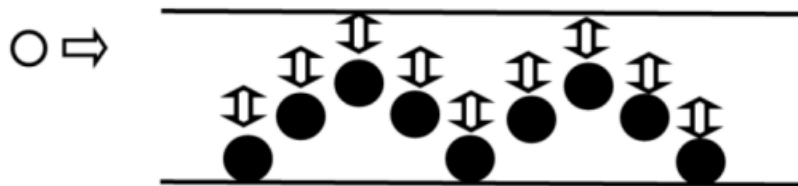


FIGURE 37

By using this toy model, we can better understand how the movement of electrons in a crystal lattice is affected by the thermal vibrations of the metal ions, and how this results in electrical resistance. This toy model serves as a valuable tool to gain a deeper understanding of how the motion of electrons in a crystal lattice connects to the thermal oscillations of metal ions, thereby causing electrical resistance. When an external electric field is applied to a crystal lattice, the electric field exerts a force on the electrons within the lattice, causing them to move in a particular direction.

As the white ball in the toy model represents the electron, this force is shown by the white ball moving in a particular direction. As the electron moves through the lattice, it collides with the metal ions they are represented by the black balls in the toy model. These collisions cause the metal ions to vibrate or oscillate around their equilibrium positions. These

vibrations increase with temperature, as thermal energy is added to the lattice. The vibrations of the metal ions create an obstacle for the electrons as they move through the lattice. This obstacle is the electrical resistance of the lattice, which opposes the flow of electric current through the metal. The resistance of the lattice is affected by various factors, including the temperature of the lattice, the strength of the electric field, and the structure of the lattice itself. By adjusting these factors, we can increase or decrease the resistance of the lattice. In summary, the toy model helps us visualize how the movement of electrons in a crystal lattice is affected by the thermal vibrations of the metal ions. These vibrations create resistance to the flow of electric current through the lattice, which can be adjusted by controlling various factors.

The electrical resistance of a crystal lattice is determined by several factors such as temperature, electric field strength and lattice structure. If we want to explain their effects in more detail, we can say the following. As the temperature of the lattice increases, the metal ions vibrate more vigorously, impeding the flow of electrons and increasing the electrical resistance of the lattice. Conversely, lowering the temperature decreases the amplitude of the thermal vibrations of the ions, which decreases the resistance of the lattice. The strength of an electric field applied to the lattice determines the force experienced by the electrons. The higher the electric field strength, the greater the force on the electrons and the higher the electrical current through the lattice. However, the collisions between the moving electrons and vibrating metal ions will still cause resistance to the flow of current. Increasing the electric field strength increases the current, but also increases the lattice heating, which in turn increases resistance due to increased thermal vibrations. The crystal lattice structure also plays a role in determining its resistance. A more regular and ordered lattice will generally have lower resistance compared to a more disordered one. This is because in a more regular lattice, the metal ions are arranged more uniformly and their vibrations are more coordinated, resulting in fewer collisions with the moving electrons.

By adjusting these factors, we can control the electrical resistance of the lattice. For example, if we increase the temperature, we can increase the resistance of the lattice, while decreasing the temperature decreases the resistance. Similarly, by increasing the electric field strength, we can increase the current flow, but also the resistance due to increased heating. Additionally, we can modify the lattice structure to optimize its electrical properties.

If the magnitude of the black ball oscillations decreases with decreasing temperature, it means that the thermal vibrations of the metal ions in the crystal lattice are decreasing. When the temperature of the lattice decreases, the amplitude of the thermal vibrations of the metal ions decreases, which leads to fewer collisions between the moving electrons and the vibrating metal ions. As a result, the damping of the oscillations decreases, and the black ball can oscillate for a longer time. This phenomenon is commonly observed in pendulum clocks, where lower temperatures lead to longer and more accurate timekeeping. Fewer collisions reduce the resistance of the metal, allowing more electrons to flow through the lattice. The relationship between temperature and resistance is typically nonlinear, but in many cases, it can be approximated by a linear relationship over a limited temperature range. For example, a pendulum clock with a metal pendulum , as shown in Figure 38 , will experience decreased damping and increased accuracy as the temperature drops. At lower temperatures, the

lattice's metal ions vibrate less, which causes fewer collisions and less resistance to the pendulum's movement, allowing for longer and more accurate timekeeping. This approximation is known as the "linear temperature coefficient of resistance" (LTC).

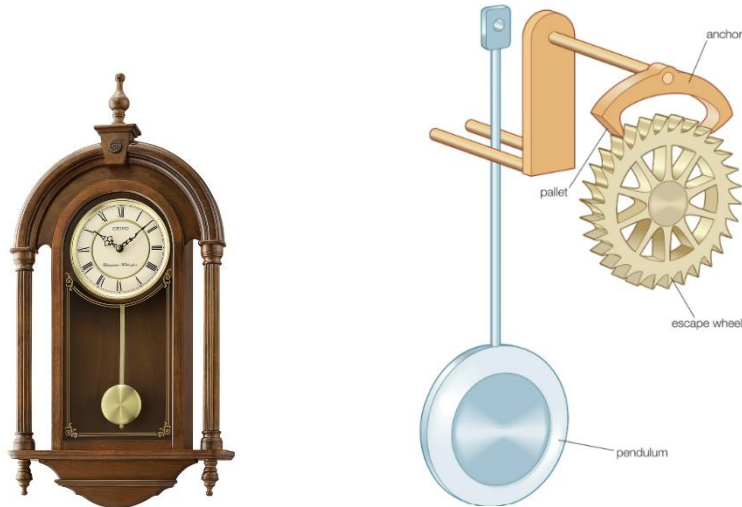


FIGURE 38

The LTC is an important parameter in many electronic devices, as it can affect their performance and stability. In addition to pendulum clocks, the LTC can be used to estimate the temperature of a material by measuring its resistance, as the resistance of a material is directly proportional to its temperature. However, it is important to note that the LTC is not constant for all materials and can vary depending on factors such as impurities, crystal structure, and other material properties. The LTC relates the change in the resistance of the metal to a change in temperature, and it is given by the equation:

$$\frac{\Delta R}{R} = \alpha \times \Delta T$$

Where ΔR is the change in resistance, R is the original resistance, α is the temperature coefficient of resistance, and ΔT is the change in temperature. The linear relationship between resistance and temperature assumes that the temperature change is small and that the material properties are not affected by the temperature. Under these conditions, we can expect to see a linear relationship between resistance and temperature, where the resistance decreases as the temperature decreases.

However, for larger temperature changes or certain materials, this assumption may not hold true and the relationship may become non-linear. Additionally, the temperature coefficient of resistance varies for different materials and can even change with temperature itself. Therefore, when using the LTC to estimate temperature, it is important to consider the specific material being measured and to take into account any potential nonlinearity in the relationship between resistance and temperature. Overall, the LTC is a useful tool for measuring temperature in certain materials, but its limitations and variations must be carefully considered.

In conclusion, decreasing the lattice's temperature causes the amplitude of the metal ions' thermal vibrations to drop, which lowers the metal's resistance. Despite the fact that the relationship between resistance and temperature is normally nonlinear, over a certain temperature range, it can be approximated by a linear relationship as shown in Figure 39.

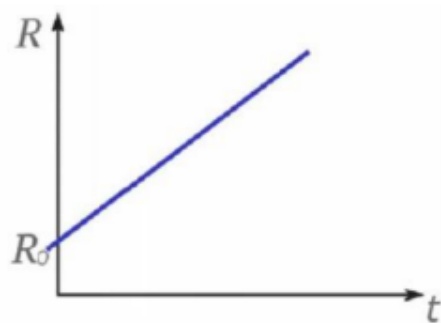


FIGURE 39

RESULT AND DISCUSSION

In general, the positively and negatively charged ions that make up ionic crystals are kept together by powerful electrostatic forces. These crystals' structural stability and physical characteristics are greatly influenced by the electrical energy contained inside them. In this work, we looked at the contributions of electrostatic energy to ionic crystals and its consequences. According to our computations, the electrostatic energy present in ionic crystals originates from the attractive interactions between ions of opposite charges and the repulsive interactions between ions of the same charge. The dominant forces at play are the attractive ones, which are dictated by Coulomb's law. These attractive forces generate a lattice energy that is usually many times larger than thermal energies, thus playing a vital role in enhancing the stability of the crystal. The strength of the electrostatic energy in ionic crystals is influenced by various factors, such as the charges carried by the ions, the distances between them, and the dielectric properties of the crystal lattice. Ionic crystals with greater ion charges or shorter distances between ions exhibit higher electrostatic energies. Furthermore, the introduction of a polarizable medium can cause changes in the dielectric constant, thereby modifying the strength of the electrostatic interactions and impacting the overall energy of the crystal. Designing materials with certain qualities requires an understanding of the electrostatic energy in ionic crystals. The electrostatic interactions may be tuned and specialized materials can be made by adjusting charges, ionic radii, and crystal shapes. An ionic crystal can be doped with impurities, for instance, to create defects and affect the charge distribution, which can change the crystal's electrical conductivity or optical absorption. In conclusion, ionic crystals' electrostatic energy is a basic factor that controls their stability and characteristics. The entire energy balance is greatly influenced by the attraction and repulsive interactions between ions, with attractive forces

predominating. Ionic charges, separation lengths, and dielectric characteristics are only a few examples of the variables that affect how much electrostatic energy there is.

Opportunities for materials engineering and the creation of new functional materials exist in the understanding and management of the electrostatic energy in ionic crystals. Deeper investigation will increase our understanding and create new opportunities for technological growth.

The Madelung constant, which is also referred to as the Madelung energy or lattice sum, is a mathematical parameter employed to assess the electrostatic energy of an unbounded one-dimensional crystal lattice. In a 1D crystal, the ions are organized in a straight line configuration, leading to a simplified geometric arrangement that facilitates the determination of the Madelung constant. To calculate the Madelung constant for a 1D crystal, the individual contributions of all ions in the lattice are summed, taking into account their charges and distances relative to a chosen reference point. The Madelung constant relies on the long-range behavior of electrostatic interactions, meaning that the impact of each ion on the constant varies depending on its specific position within the crystal lattice. Calculating the Madelung constant necessitates meticulous examination of the crystal's arrangement, encompassing the lattice's periodicity and symmetry. To find the Madelung constant, a series is produced and the Maclaurin series is assisted for this series. The specific arrangement and distribution of charges among ions influence the resulting Madelung constant for a 1D crystal, which can take on positive, negative, or potentially divergent values. Comprehending the significance of the Madelung constant is essential for examining the stability, electronic characteristics, and behavior of 1D crystal structures. It offers valuable insights into the potency of electrostatic interactions and their influence on the total energy of the crystal system. Additionally, the Madelung constant holds fundamental importance in theoretical computations, enabling the modeling of charge distributions, anticipation of lattice energies, and exploration of phase transitions within 1D crystal systems.

All the information about the Madelung constant in 1 dimension mentioned above is also valid for the Madelung constant in 2 dimensions. However, as seen in the evaluation of problems, no exact value was found for the Madelung constant in 2 dimensions. While the Madelung constant in 1 dimension was found to be approximately 1.38, the Madelung constant in 2 dimensions was found as (1.3571+...). Thus, a numerical evaluation was made for the Madelung constant in 2 dimensions.

The equivalent capacitance varies as the number of nodes increases. In 4 node capacitors the equivalent capacitance was 105.7 micro-farad. in the 16 node capacitor, however , the equivalent capacitance was 57.4 micro-farad.Between 4 nodes and 16 nodes, it showed an approximately 45.69% decrease , which is a significant drop. In 64 node capacitors, the equivalent capacitance was 37.7 microfarad, which doesn't have the same drop as the previous one. In the 128 node capacitor, however, the equivalent capacitance was 27.8 microfarad, showing again a less drop than the previous one . We can conclude from this that the drop in capacitance of the node decreases as the drop percent changes frequently. In the 256 node capacitor, the equivalent capacitance was 28.7 microfarad. The raise in 256 nodes shows that, in fact, the node amount can actually alter the drop and the

raises. This indicates that the capacitance of a node is not a fixed value, but rather a dynamic one that changes with the voltage applied to it. It is important to note that this phenomenon is not limited to the 256 node capacitor but can be observed in other larger node capacitors as well. Understanding this behavior is crucial for designing circuits that rely on stable capacitance values.

Van der Waals bonding, also known as molecular bonding, plays a vital role in maintaining the structural stability and physical properties of inert gas crystals. Unlike other elements, such as those involved in chemical bonding, inert gas atoms exist independently rather than forming traditional bonds. However, despite the absence of conventional bonding, these atoms possess weak attractive forces referred to as Van der Waals forces. These forces emerge from momentary variations in electron distribution, resulting in temporary dipoles in nearby atoms. These temporary dipoles induce dipole moments in adjacent atoms, leading to an attractive force between them. Although individually feeble, the cumulative impact of these intermolecular forces is significant enough to generate cohesive forces, which hold the atoms together within a solid crystal lattice. The strength of Van der Waals bonding relies on the atomic polarizability and size of the inert gas atoms. This distinctive bonding mechanism contributes to the low melting and boiling points of inert gases, as well as their resistance to chemical reactions.

The Lennard-Jones potential equation is a mathematical formula utilized to depict the interactions between atoms or molecules in a given system. It finds extensive application in molecular dynamics simulations and the investigation of diverse physical and chemical phenomena.

Using the Lennard-Jones potential energy equation, the formula for the force in terms of distance r is found. The connection between potential energy and force is a fundamental concept in physics. The force exerted on an object is directly linked to the slope of its potential energy. In mathematical terms, force (F) can be described as the negative rate of change of potential energy (U) with respect to position (r).

$$F = \frac{-dU}{dr}$$

This relationship arises from the principle of conservative forces, where the work done by a force solely depends on the initial and final positions, independent of the path taken. Potential energy represents the stored energy within a system, while force represents how this energy changes as the object's position varies.

Investigating the extrema, both minima and maxima, of functions $U(r)$ and $F(r)$ offers valuable insights into their behavior and characteristics. Extrema represent the highest or lowest values that these functions attain within a given range. To identify the extrema of $U(r)$, one can analyze its derivative, dU/dr . Points where dU/dr is zero or undefined suggest potential extrema. A positive second derivative, d^2U/dr^2 , at these points indicates a minimum, while a negative second derivative suggests a maximum. Similarly, for the force function $F(r)$, extrema can be examined by studying its derivative, dF/dr . Points where dF/dr is zero or undefined may indicate extrema. A positive second derivative signifies a local minimum, while a negative second derivative implies a local maximum. The investigation of

extrema in $U(r)$ and $F(r)$ facilitates the understanding of critical points, equilibrium positions, stability, and the overall behavior of the systems associated with these functions.

The equilibrium distance (r_{eq}) in the Lennard-Jones potential is a critical factor in determining the stable arrangement of interacting particles. It represents the distance where the potential energy is minimized and the net force between particles is close to zero. At r_{eq} , the attractive and repulsive forces balance out, leading to a stable configuration. Any deviations from r_{eq} result in a net force that drives the particles either closer or farther apart, causing changes in potential energy. The specific value of r_{eq} depends on the parameters of the Lennard-Jones potential, including the depth and characteristic length of the potential well. A thorough understanding and characterization of the equilibrium distance are vital for investigating the stability, properties, and phase transitions of systems governed by the Lennard-Jones potential. When necessary operations are done, the r_{eq} is found 1.1225σ .

Determining the Cartesian components of the gradient vector for the Lennard-Jones potential energy function, $U(r)$, is a crucial step in comprehending the spatial distribution of forces within the system. The gradient vector denotes both the magnitude and direction of the steepest increase in potential energy. By computing the partial derivatives of $U(r)$ with respect to each Cartesian coordinate (x , y , and z), we can derive the corresponding Cartesian components of the gradient vector. These components offer valuable insights into the strength and orientation of the forces acting on the particles. The Lennard-Jones potential energy function exhibits radial dependence, where the force and potential energy predominantly depend on the inter-particle distance. Consequently, the Cartesian components of the gradient vector elucidate how forces vary along the x , y , and z axes, contingent upon the specific particle arrangement. Understanding the Cartesian components of the gradient vector is indispensable for characterizing the spatial distribution of forces and acquiring a deeper understanding of the behavior and properties of systems governed by the Lennard-Jones potential.

The determination of the work (W) carried out by the Lennard-Jones force when transferring an electrical charge (e) from the initial position ($r = \sigma$) to infinity is a crucial aspect in the analysis of energy interactions within the system. The Lennard-Jones force arises from intermolecular interactions and is characterized by the Lennard-Jones potential. To calculate the work, it involves integrating the force with respect to distance as the charge is moved from σ to infinity. When operations are done, the result will be zero.

$$W = \int \overrightarrow{F(r)} \cdot \overrightarrow{dr}$$

As the Lennard-Jones potential exhibits spherical symmetry, the work performed in transferring the charge depends on the intermolecular distance and encompasses both attractive and repulsive force components. A comprehension of the work accomplished by the Lennard-Jones force in this process provides valuable insights into the energy landscape,

system stability, and interactions. It facilitates the quantification of the energy requirements for charge movement and finds applications in molecular dynamics, materials science, and the understanding of particle behavior in diverse physical and chemical systems.

It is considered a simplified "toy" model that represents the interaction between electrons in a metal and the vibrating ions of the crystal lattice. It is assumed that the magnitude of the black ball oscillations decreases with decreasing temperature. As the temperature of the lattice rises, the oscillations of the metal ions become more intense, impeding the movement of electrons, and causing an increase in the electrical resistance of the lattice. Conversely, decreasing the temperature reduces the magnitude of the thermal vibrations of the ions, resulting in a decrease in lattice resistance. The force experienced by the electrons is determined by the strength of the applied electric field. A higher electric field strength leads to a stronger force on the electrons and an increase in electrical current flowing through the lattice. However, collisions between the mobile electrons and the vibrating metal ions still contribute to resistance in the current flow. Amplifying the electric field strength boosts the current, but it also raises lattice heating, leading to an increase in resistance due to heightened thermal vibrations. The resistance of the crystal lattice is also influenced by its structural arrangement. A more orderly and uniform lattice generally exhibits lower resistance compared to a more disordered one. This is because a well-organized lattice ensures the metal ions are evenly spaced and their vibrations are more coordinated, resulting in fewer collisions with the moving electrons. The correlation between temperature and resistance is typically nonlinear; however, it can often be approximated by a linear relationship within a specific temperature range. This approximation is referred to as the "linear temperature coefficient of resistance" (LTC). The equation $\Delta R/R = \alpha\Delta T$, which relates resistance to temperature, assumes that the temperature change is minor and that the material's properties remain unaffected by temperature. In such circumstances, we would observe a linear correlation between resistance and temperature, with resistance decreasing as temperature decreases. However, when dealing with significant temperature variations or materials exhibiting more intricate characteristics, the association between resistance and temperature may not follow a linear pattern. While the typical relationship between resistance and temperature is non-linear, it is possible to approximate it using a linear relationship within a specific temperature range.

CONCLUSION

In conclusion, it is observed that the result of the equivalent resistance obtained in the laboratory environment and the result of the equivalent resistance obtained with the simulation program are different. Differences between the measured equivalent resistance in a laboratory and the simulated results can stem from multiple factors. When conducting measurements in a lab, inherent flaws and uncertainties in the measurement process can play a role. Imperfect connections, resistance in the wires, and errors in measurement techniques can introduce discrepancies in the recorded values. Moreover, environmental conditions such as temperature and humidity can impact the electrical components, thereby modifying their resistance. These variations can result in disparities between the measured equivalent resistance and the anticipated theoretical value.

Likewise, differences between results can be seen in equivalent capacitance. The disparity between the measured capacitance in a laboratory and the value obtained from a simulation program can be ascribed to various factors. In a real-world setting, practical limitations and imperfections in the experimental setup, such as stray capacitance, resistance in circuit components, imprecise measuring instruments, and external interference, can introduce errors and uncertainties, resulting in deviations from the measured capacitance. Conversely, simulation programs typically assume ideal conditions and flawless components, disregarding real-world imperfections. They rely on mathematical models and algorithms to anticipate circuit behavior, which may not fully encompass the complexities of the physical environment. Consequently, simulation outcomes may diverge from actual measurements due to the simplifications inherent in the virtual representation of the circuit.

In contrast, simulation programs aim to simulate and analyze circuits or systems theoretically. These programs employ mathematical models and algorithms to compute the equivalent resistance by considering the properties of the circuit components. Although simulations strive for accuracy, they make assumptions and rely on idealized conditions that may not fully capture the intricacies and imperfections found in real-world situations. The precision of the simulation results is contingent upon the accuracy of the models, the accuracy of the algorithms used, and the inputs provided by the user. Moreover, disparities can occur due to limitations inherent in the simulation program. Simplifications or assumptions made during the modeling phase, numerical approximations, or the exclusion of specific physical effects can all contribute to differences between the simulated equivalent resistance and the actual measured value. It is crucial to acknowledge that although there might be variations between laboratory measurements and simulation results, both methods serve their distinct purposes. Laboratory measurements offer direct experimental evidence and consider the intricacies of real-world conditions. On the other hand, simulations provide a theoretical understanding and the capability to efficiently explore various scenarios. Integrating the insights gained from both experimental and simulation approaches can lead to a more comprehensive comprehension of the behavior of electrical circuits and systems.

REFERENCE LIST

- [https://chem.libretexts.org/Bookshelves/Inorganic_Chemistry/Map%3A_Inorganic_Chemistry_\(Housecroft\)/06%3A_Structures_and_Energetics_of_Metallic_and_Ionic_solids/6.13%3A_Lattice_Energy_-_Estimates_from_an_Electrostatic_Model/6.13E%3A_Madelung_Constants](https://chem.libretexts.org/Bookshelves/Inorganic_Chemistry/Map%3A_Inorganic_Chemistry_(Housecroft)/06%3A_Structures_and_Energetics_of_Metallic_and_Ionic_solids/6.13%3A_Lattice_Energy_-_Estimates_from_an_Electrostatic_Model/6.13E%3A_Madelung_Constants)
- <https://www.youtube.com/watch?v=sqp1GBO8LAU>
- https://en.wikipedia.org/wiki/Lennard-Jones_potential
- <https://www.youtube.com/watch?v=aAvxoP77nOY>
- <https://math.stackexchange.com/questions/1742524/numerical-force-due-to-lennard-jones-potential>
- [https://chem.libretexts.org/Bookshelves/Physical_and_Theoretical_Chemistry_Textbook_Maps/Supplemental_Modules_\(Physical_and_Theoretical_Chemistry\)/Physical_Properties_of_Matter/Atomic_and_Molecular_Properties/Intermolecular_Forces/Specific_Interactions/Lennard-Jones_Potential#:~:text=The%20Lennard%2DJones%20Potential,-The%20Lennard%2DJones&text=V%20is%20the%20intermolecular%20potential,is%20zero%20\(Figure%201\)](https://chem.libretexts.org/Bookshelves/Physical_and_Theoretical_Chemistry_Textbook_Maps/Supplemental_Modules_(Physical_and_Theoretical_Chemistry)/Physical_Properties_of_Matter/Atomic_and_Molecular_Properties/Intermolecular_Forces/Specific_Interactions/Lennard-Jones_Potential#:~:text=The%20Lennard%2DJones%20Potential,-The%20Lennard%2DJones&text=V%20is%20the%20intermolecular%20potential,is%20zero%20(Figure%201))
- <https://onlinelibrary.wiley.com/doi/full/10.1002/jcc.26368>
- <https://www.allaboutcircuits.com/textbook/direct-current/chpt-12/temperature-coefficient-resistance/>
- https://www.youtube.com/watch?v=J3_WL2X92_w&t=456s